AFCRL-63-20(a)

SEMICONDUCTOR DEVICE CONCEPTS

General Electric Company
General Electric Research Laboratory
Schenectady, New York

Scientific Report No. 2A

AF 19(628)-329
Project 4608
Task 460804
November 30, 1962

Prepared for

ELECTRONICS RESEARCH DIRECTORATE
AIR FORCE CAMBRIDGE RESEARCH LABORATORIES
OFFICE OF AEROSPACE RESEARCH
UNITED STATES AIR FORCE
BEDFORD, MASSACHUSETTS

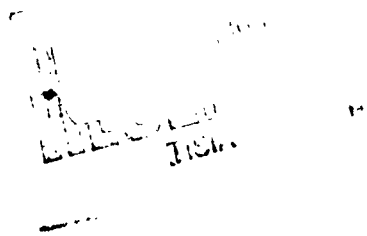

Requests for additional copies by Agencies of the Department of Defense, their contractors, and other Government agencies should be directed to the:

ARMED SERVICES TECHNICAL INFORMATION AGENCY
ARLINGTON HALL STATION
ARLINGTON 12, VIRGINIA

Department of Defense contractors must be established for ASTIA services or have their "need-to-know" certified by the cognizant military agency of their project or contract.

All other persons and organizations should apply to the:

U. S. DEPARTMENT OF COMMERCE
OFFICE OF TECHNICAL SERVICES
WASHINGTON 25, D.C.

TABLE OF CONTENTS

	Page
Abstract	3
A. The Effect of Elastic Strain on Interband Tunneling in Sb-Doped Germanium	5
I. Introduction	5
II. Theoretical Considerations	7
III. Experimental	9
IV. Interpretation	12
1. Stress Tunneling Coefficient Beyond the Kane Kine	14
2. Stress Coefficient in the Indirect Tunneling Range	18
3. Comparison of Absolute Magnitudes of Tunneling Parameters with Theory	26
V. Summary and Conclusion	28
Table	31
References	32
Figure Captions	35
Figures	37
B. Carrier Mobility and Shallow Impurity States in ZnSe and ZnTe	44
I. Introduction	44
II. Experimental	46
III. Results and Discussion	48
1. ZnTe - Impurity and Native Defect Levels	50
2. ZnSe - Donor Levels	57
3. Mobilities of ZnTe and ZnSe	60
IV. Conclusion	68
Table	71
References	72
Figure Captions	77
Figures	79
C. Light Emission From $GaAs_{1-x}P_x$ and GaSb Junctions	85
Contributors	87
Papers Sponsored Under Contract	87

SEMICONDUCTOR DEVICE CONCEPTS

Abstract

The effects of uniaxial compression and of hydrostatic pressure on the direct and indirect tunneling processes in germanium tunnel diodes have been studied experimentally under forward and reverse bias at 4.2°K and compared with Kane's theory. The diodes were formed by alloying indium doped with 3/8 weight per cent gallium on (100) and (110) faces of germanium bars containing an antimony concentration of $5.5 \times 10^{18}/cm^3$. The first order change of the tunneling current with stress was measured at fixed bias voltages. For biases smaller than 8 mv the current is direct and not affected by the relative shifts of the (111) conduction band valleys. In the bias range of indirect tunneling the anisotropic tunneling from the (111) valleys was observed in agreement with theory. In the range of direct tunneling to the (000) conduction band, the current change is correlated with the stress induced change of the direct band gap and of the energy separation between the (111) and (000) conduction bands. This separation was found to be 0.160 ± 0.005 ev at zero stress in agreement with optical measurements on degenerate germanium. Some details of the bias dependence of the pressure effect including some fine structure at small biases remain unexplained.

Electrical transport measurement have been made on p-type ZnTe and n-type ZnSe. In ZnTe crystals doping with Cu, Ag and Au produces acceptor levels at 0.15, 0.11, and 0.22 ev respectively. An acceptor with an ionization energy of 0.048 ev was found in the undoped crystals and is identified as the first charge state of the Zn-vacancy. A shallow

donor state, at approximately 0.01 ev below the conduction band, was found in n-type ZnSe. It also proved possible to prepare degenerate ZnSe. The scattering mechanisms limiting the lattice mobilities of both materials were considered. It was found that the polar interaction with the longitudinal optical phonons dominates the scattering of electrons in ZnSe. This mechanism probably also predominates in the scattering of the holes in ZnTe. However, the non-polar interaction with the optical modes could also contribute significantly if the appropriate coupling parameter is larger than we presently believe.

Luminescence from p-n junctions constructed from the mixed crystal $GaAs_{1-x}P_x$ and from GaSb has been studied. Visible red radiation is produced by the former, but at present the efficiency is poor and the junction profile is quite irregular, presumably because of poor crystal structure. Attempts to produce coherent radiation from these junctions has thus far been unsuccessful.

SEMICONDUCTOR DEVICE CONCEPTS

A. The Effect of Elastic Strain on Interband Tunneling in Sb-Doped Germanium (H. Fritzsche and J. J. Tiemann)

The research reported here evolved from experiments carried out under Contract AF 19(604)-6623 which preceded the present one. These early investigations were described in Reports 3A and 4A of that contract, dated 23 December 1960 and 28 March 1961. In view of this history it seems appropriate to present here a report of this work which has now reached a satisfactory conclusion.

I. INTRODUCTION

As a result of extensive experimental and theoretical efforts, the main features of the tunneling process in Esaki tunnel diodes[1] have been clearly established. However, since it is difficult to assess the validity of some of the simplifying assumptions and approximations which underlie our present theoretical understanding of this process, it is not clear to what extent theexisting theories[2,3] should explain the finer details of the experimental observations. This probelm is particularly difficult to resolve because tunnel diodes can only be made in highly impure materials. This fact precludes the possibility of ever performing a tunnel diode experiment under very ideal conditions. It is hoped that some of these difficulties can be alleviated by performing a series of experiments upon each diode. In this paper we discuss measurements of the effect of hydrostatic pressure and of uniaxial compression on the tunneling current of germanium tunnel diodes at helium temperatures. A subsequent paper will report the temperature dependence of the tunneling current of the same diodes.

The effects of elastic strain will strongly depend on the effective mass anisotropies and on the deformation potentials of the relevant band extrema. Most of these quantities are known for germanium.[4] Furthermore, in germanium, two types of tunneling have been observed,[5,6] and theoretical expressions for both types have been derived.[3] These two tunneling processes are (1) direct tunneling and (2) indirect or phonon assisted tunneling. The relative proportion of the current carried by these two processes depends on the temperature, the bias voltage, and on whether As, P or Sb is used as the donor impurity.[5] Although the mechanism is not understood theoretically at present, direct tunneling predominates in As- and P-doped diodes at all temperatures and biases. In Sb-doped diodes, on the other hand, one observes at helium temperatures several distinct bias regions in which one or the other of these processes is dominant. This material has the advantage that both direct and indirect tunneling are observable in separate bias ranges in a single diode.

This is important because there is considerable experimental uncertainty as regards the details of the impurity distribution within the junction itself. By measuring both types of tunneling in one sample, this uncertainty does not affect the conclusions. Antimony-doped germanium tunnel diodes have the additional advantage that the unambiguously direct tunneling to the (000) minimum in the conduction band is much more clearly observed.[6,7]

The main effect of elastic strain on the tunneling current arises from the shifts in energy of the conduction band valleys with respect to the valence band. Hydrostatic pressure causes all of the conduction

band valleys to rise in energy, but the (000) valley moves faster than the (111) valleys.[8] In addition, shear stress can shift the (111) valleys with respect to one another.[9] These effects can be quantitatively calculated by applying deformation potential theory to the expressions for the tunnel current derived by Kane.[3] The calculated behavior is in good qualitative agreement with the main features of the experimental data.

II. THEORETICAL CONSIDERATIONS

According to Kane's theory,[3] the tunneling current flowing from a single valley in the conduction band to the valence band is given by

$$I_d = C_d\, D \exp(-\alpha) \text{ with } \alpha = \lambda_d E_g^{3/2} m^{*1/2}/F \qquad (1)$$

when the transition is direct, i.e. when the conduction and valence band extrema occur at the same wave number k. It is given by

$$I_i = C_i\, D \exp(-\beta) \text{ with } \beta = \lambda_i E_g^{3/2} m^{*1/2}/F \qquad (2)$$

when the transition is indirect, i.e. when the band extreme occur at different k.

In Eqs. (1) and (2) E_g is the appropriate band gap, $m^* = (1/m_{hx} + 1/m_{ex})^{-1}$ is the reduced effective mass in the tunneling direction. The quantities C and λ are given by Kane. The average junction field is given by

$$F = [2\pi n^* (E_g + \zeta_n + \zeta_p - eV)/\kappa]^{1/2} \qquad (3)$$

where $n^* = np/(n+p)$ is the reduced doping constant, κ is the dielectric constant, ζ_n and ζ_p are the Fermi level penetrations into the conduction band and the valence band, respectively, and E_g is the smallest band gap. In Eq. (2) the energy of the phonon which is required to conserve wave

number in the indirect transition has been neglected in the exponential factor. The phonon energy has to be considered in the density of states factor D, however, as will be discussed later. The density of states factor is given in Kane's notation by

$$D = \int [1 - \exp(-2E_s/\bar{E}_i)]\,[f_1(E_1) - f_2(E_2)]\,dE. \qquad (4)$$

When there is more than one valley in the conduction band, or more than one valence band, the total current will be a sum over all combinations of conduction band and valence band extrema which can contribute. Because of the exponential dependence on the reduced mass appearing in Eqs. (1) and (2), however, this sum for germanium can be reduced to only those transitions which involve the light hole band. Furthermore, since the conduction band valleys in germanium are quite anisotropic, and since the tunneling probability depends only on the effective mass along the direction of tunneling[10] the current contributions of the four (111) valleys will in general be different.

That part of the applied stress which is associated with a volume change affects the tunnel currents primarily through E_g and m^*, which appear in the exponents of Eqs. (1) and (2). The variations of these quantities with stress can be estimated from the known pressure coefficients of the band gaps.

The pure shear part of the stress causes the conduction band valleys to shift in energy with respect to one another in such a way that their average energy is unchanged. Therefore, for the shifts in valley energies to produce a current change which is linear in stress, it is necessary (a) that the degeneracy of the valleys be removed by

shear, and (b) that the current contributions of the valleys which are raised in energy be unequal to the contributions from those which are lowered.

If the electric field is in a [100] direction, all (111) valleys have the same effective mass component in the field direction. For such a diode an energy shift of the valleys should not produce a current change which is linear in shear stress.[11] If the electric field is in the [110] direction, however, two valleys (those along $[1\bar{1}1]$ and $[1\bar{1}\bar{1}]$) have reduced effective masses along the field direction $m_1^* = m_2^* = \left(\frac{1}{m_{te}} + \frac{1}{m_h}\right)^{-1} = 0.027\ m_o$; while the two other valleys (along [111] and $[11\bar{1}]$) have reduced effective masses $m_3^* = m_4^* = \left(\frac{1}{3m_{te}} + \frac{2}{3m_{\ell e}} + \frac{1}{m_h}\right)^{-1} = 0.034\ m_o$, where m_{te}, $m_{\ell e}$, and m_h are the principal electron masses and the light hole mass, respectively. Even though these effective masses differ by only about 25%, the currents themselves will differ by a large factor because of the exponential dependence. In our samples, for example, the exponent is about equal to 16. This leads to a factor of 6 difference in the currents. Such a diode will exhibit a first order stress coefficient for a shear which causes the similar valleys to move in the same direction. (On the other hand, a shear which raises one valley of each pair while lowering the other valley will have no first order shear dependence.)

III. EXPERIMENTAL

Our experimental diodes were chosen so that they are as identical as possible except that one sample has the electric field along the [001] axis and the other along [110]. For both samples the uniaxial stress direction was $[1\bar{1}0]$. The samples were in the form of rectangular

bars with the long dimension along [1$\bar{1}$0] and the short dimensions along [110] and [001]. Two diodes were alloyed near the center of each bar on opposite faces. It was found to be necessary to do this because it was impossible to avoid flexing the bars slightly. Since flexure causes equal and opposite stresses on opposite faces, the average of the results obtained from these diodes is independent of flexure.

The starting material was pulled along the [110] axis from a melt containing 6% Sb by weight. After orientation by x-rays, the crystal was cut into wafers. These wafers were reoriented and cut into bars with the long dimension along [1$\bar{1}$0] and the short dimensions along [110] and [001]. From resistivity and Hall effect measurements, the Fermi level penetration of our samples was calculated to be ζ_n = .020 ± .002 volts. The diodes were formed by alloying indium dots doped with 3/8 weight % gallium on the appropriate faces. Double contact wires were attached to the dots and the samples were etched to remove the perimeter of the junctions. (This was done because the perimeter has the wrong orientation.) The diameter of a typical diode dot was about 0.05 cm.

The Fermi level on the p-type side was estimated to be approximately .140 ± .020 ev. No direct measurements were made to confirm this estimate, but since none of our conclusions is sensitive to the choice of ζ_p, as long as $\zeta_p > \zeta_n$, the accuracy of the estimate is unimportant.

Uniaxial compressional stresses X varying between 5×10^7 and 5×10^8 dynes/cm^2 were applied parallel to the [1$\bar{1}$0] direction at temperatures between 1.5 and 4.2°K. The stress tunneling coefficient

defined as $\pi = \Delta I/IX$ averaged over the two opposed diodes was found to be independent of stress and of temperature within these ranges. The stress tunneling coefficients were measured at fixed bias voltages. In order to minimize the effect of series resistances due to the leads and the sample, the bias was measured potentiometrically using one pair of the double contact wires attached to the diode and to an ohmic contact in close proximity of the diodes while the current was passed through the other pair of contact wires. Liquid helium was used as the pressure transmitting fluid for the hydrostatic pressure measurements. These were extended up to $p = 10^3$ psi.

Fig. 1 shows the stress tunneling coefficient as a function of bias for the two samples. In sample 1 the diodes are on the (001) faces. This sample should, therefore, not respond to the shear induced shifts of the conduction band valleys. In sample 2 the diodes are on the (110) faces. The difference between these two curves is due mainly to the nonequivalence of the two pairs of valleys for tunneling in the [110] direction and the fact that the shear part of the applied stress causes these pairs to move in opposite directions.

The same figure shows the hydrostatic pressure coefficient of sample 1 at 4.2°K. In order to make a direct comparison with the uniaxial compression data possible $\pi_p = \Delta I/3Ip$ was plotted. The difference between the uniaxial and the hydrostatic pressure coefficients of sample 1 is due to the shear-induced effective mass changes of the electrons and light holes in the tunneling direction.

The I-V characteristic of one of the diodes of sample 2 is plotted on Fig. 2. The two diodes were so closely matched that their characteristics did not differ by more than 10°/o over the whole voltage range. The characteristic has the shape typical for indirect tunneling.[5] Only a very small current can flow until the bias is large enough to permit the emission of a low energy phonon needed for wave number conservation in the tunneling process from a (111) conduction band valley to the (000) valence band. The current increases again when a higher energy phonon of the same wave number can be emitted. The phonons have been identified previously[5] as the TA and LA [111] phonons which have the energies 0.0076 eV and 0.028 eV, respectively.[12]

The I-V characteristic of the same diode is plotted on a different scale in Fig. 3 in order to show the rapid increase of the reverse current at a bias voltage of about -140 mV. This so-called Kane kink occurs[6] when the back bias is large enough to move the higher lying conduction band edge at k = 0 on the n-type side below the Fermi level in the valence band on the p-type side and thus to allow a large direct tunneling current to flow. The relative position of the bands is shown schematically in Fig. 4 for a reverse bias beyond the Kane kink.

IV. INTERPRETATION

Comparing Figs. 1 and 2 one sees that the stress coefficients π of the two samples differ greatly in the bias range of indirect

tunneling, i.e. for $-135 < V < -8$ mV and $V > 8$ mV. We shall interpret this difference as being due to the shear induced shifts of the (111) valleys and the nonequivalence of the two pairs of valleys for tunneling in the [110] direction. In the small bias range -8 mV $< V < +8$ mV a very small current flows. This must be due to a direct tunneling process since the energy difference between the Fermi levels on the n-type and p-type sides is too small for the emission of a phonon. Although the detailed nature of this direct tunnel current is not known, the relative magnitude of this component in Sb, P, and As-doped germanium tunnel diodes indicates[6] that the origin of this direct process is related to the impurity cell potentials of the n-type impurities.[13] The fact that the stress coefficients of the two samples are practically identical in this range indicates furthermore that this direct tunneling process cannot be associated with the density of states and the band edge energies of the individual (111) valleys.

As can be seen from Fig. 1, both samples exhibit a sharp rise in the stress coefficient at about 140 mV reverse bias. This effect is obviously associated with the onset of direct tunneling into the (000) conduction band. All three curves are nearly the same beyond the Kane kink. This one expects since the (111) valley contribution to the current is negligible in this range.

In the following we shall attempt a quantitative comparison between the experiments and Kane's theory.

1. Stress Tunneling Coefficient Beyond the Kane Kink

One expects the onset of direct tunneling to the (000) conduction band to occur at a reverse bias voltage

$$V_k = -[E_g(000) - E_g(111) - \zeta_n]/e. \qquad (5)$$

Since the pressure coefficient for the direct gap $E_g(000)$ is larger than that for the indirect gap $E_g(111)$,[8] that part of the uniaxial compression X which corresponds to a hydrostatic pressure $p = X/3$ causes the onset voltage V_k to increase. This results in an anomalously large negative value of $\Delta I/I$. As one goes to higher reverse bias, this contribution becomes relatively unimportant and the stress coefficient approaches the value determined by the stress-induced changes of $E_g(000)$ and the combined electron and hole effective mass $m^*(000)$. Figure 1 shows that these changes are determined mainly by the hydrostatic pressure part of the stress. The shear part does not change $E_g(000)$. It deforms, however, the effective mass spheres, which gives rise to a small contribution which is different for the two diode orientations.

Beyond the Kane kink the tunnel current is the sum of the direct current I_d and the indirect current I_i (see Fig. 4). Following Kane one has

$$I_d = C_d\, D(V - V_k) \exp(-\alpha) \qquad (6)$$

with

$$\alpha = \lambda_d E_g^{1/2}(000)\left[m^*(000)\right]^{1/2}/F \tag{7}$$

and

$$D(V-V_k) = e(V-V_k) + \frac{E_g(000)}{4\alpha}\left\{1-\exp\left[\frac{4\alpha e}{E_g(000)}(V-V_k)\right]\right\} . \tag{8}$$

The relative change of the tunnel current is

$$\frac{\Delta I}{I} = \frac{\Delta I_d + \Delta I_i}{I_d + I_i} . \tag{9}$$

It can be seen from Fig. 4 that beyond the Kane kink the indirect current is an appreciable fraction of the total current only over a small bias range. For the purpose of explaining the data we can therefore use for I_i and ΔI_i in Eq. (9) the extrapolations of the indirect current curves into the bias range beyond the Kane kink.

For the change of the direct current one obtains from Eqs. (6) and (7), neglecting the relatively minor change of C_d,

$$\Delta I_d = I_d \frac{1}{D}\frac{dD}{dV_k}\Delta V_k - \alpha\left[\frac{3}{2}\frac{\Delta E_g(000)}{E_g(000)} + \frac{1}{2}\frac{\Delta m^*(000)}{m^*(000)} - \frac{\Delta F}{F}\right]. \tag{10}$$

The first term in Eq. (10) is responsible for the sharp maximum of the stress coefficient near V_k, and the second term determines its asymptotic value at large reverse bias. The quantity ΔV_k is

$$\Delta V_k = -(\Xi_{000} - \Xi_{111})\frac{X}{3} \tag{11}$$

where $\Xi_{000} = 12 \times 10^{-12}$ volt cm^2/dyne and $\Xi_{111} = 5 \times 10^{-12}$ volt cm^2/dyne are the pressure coefficients for the direct and the indirect band gap, respectively.[8]

Before one can calculate the theoretical bias dependence of the stress coefficient it is necessary to estimate α and the value of $\Delta m^*(000)/m^*(000)$. The shear contribution to the latter quantity depends on the field direction and hence is different for our two samples. Its magnitude cannot be obtained without knowing the various deformation potentials which determine the stress-induced changes of the effective mass tensors at the zone center. Figure 1 shows, however, that the shear contribution is small. The relative change of the reduced mass caused by the hydrostatic pressure can be estimated from

$$\Delta m^*(000)/m^*(000) = \Delta E_g(000)/E_g(000) \quad . \tag{12}$$

since the masses involved are mainly determined by the interaction between the light hold band and the conduction band at the zone center.[14] The quantity α was then determined by fitting Eq. (10) and the experimental hydrostatic pressure curve of sample 1 at large reverse bias. From this fit, the value $\alpha = 17.6$ was obtained for $V = -300$ mV.

As an independent check, the bias dependence of the direct tunnel current itself was compared with Eqs. (6) and (7) using this α. The comparison with experiment is shown in Fig. 5. The constant factor C_d of Eq. (6) was chosen to fit the magnitudes of the measured and the calculated current. It is seen that this value of α predicts the shape of the I-V characteristic

quite well. This agreement was not noted by Morgan and Kane[6] because they assumed the junction field F did not change with bias. Even though F varies by only about 10°/o, the value of the exponential factor varies by a factor of 6 over the bias range of interest.

The theoretical stress coefficient is compared with experiment in Fig. 6. It is seen that there is good qualitative agreement except that the theoretical maximum is sharper than the experimental curve. There are several effects which will cause a smearing out of the theoretical curve. (1) Thermal fluctuation will cause about a 1.5 mV broadening. (2) Random fluctuations of the impurity concentrations on a microscopic scale will cause local fluctuations in ζ_n. These will correspond to a range of V_k values rather than a unique value as was assumed. (3) There may also be a non-uniform built-in stress in the diodes. Since $E_g(000)$ and $E_g(111)$ depend differently on stress, this would also cause a spread in V_k.

For pure germanium $E_g(000) - E_g(111) = 144$ mV.[15] For our samples, V_k should therefore occur at 124 mV. The observed V_k is clearly larger than 136 mV. This discrepancy may be due to a depression of the (111) conduction band relative to the (000) conduction band due to the large impurity concentration[16] or it may be due to a permanent strain at the junction caused by the difference in lattice constant of the n-type and the p-type regions, or possibly by the difference in the thermal expansion coefficient of the dot material and the germanium.

2. Stress Coefficient in the Indirect Tunneling Range

Except for the narrow voltage region at zero bias (see Fig. 2) the tunneling is almost entirely indirect for $V_k < V$. In this bias range the stress coefficients of the two samples differ strongly. This difference is due to the fact that in sample 1 all four valleys are equivalent with respect to the junction field direction, whereas in sample 2 the two pairs of valleys which are shifted with respect to one another by shear have different effective mass components in the field direction.

The difference between the hydrostatic and the uniaxial stress coefficient of sample 1 (see Fig. 1) is due to the shear-induced changes of the effective mass components in the field direction. It is interesting to note that these changes are of appreciable magnitude. We find $\frac{1}{m^*}\frac{dm^*}{dX} \approx 5 \times 10^{-12}$ cm^2/dyne. Since m^* is the reduced mass we cannot separate the contributions of the light hole mass and of the (111) electron mass. The fact that the shear dependence of the current beyond the Kane kink is quite small allows us to conclude that either the effective mass deformation occurs mostly on the (111) ellipsoids or that there is an accidental cancellation of the deformations of the light holes and the (000) conduction band extremum.

The bias dependence of the hydrostatic pressure coefficient shows a clearly resolved structure at small bias voltages which is symmetric with respect to the forward and reverse bias direction.

The value of the pressure coefficient $\pi_p = \Delta I/3Ip$ is about $\pi_p = -7.5 \times 10^{-11}$ cm^2/dyne in the small bias range of direct tunneling. π_p changes to -4×10^{-11} cm^2/dyne at V = $\pm$ 6 mV before it reaches a constant value of -5.5×10^{-11}. Near V = $\pm$ 30 mV, which is the onset of the LA phonon, π_p changes again to about $\pi_p = -6.5 \times 10^{-11}$ cm^2/dyne. This structure is also indicated although not as clearly by the uniaxial stress coefficient of sample 1. It is to be expected that the stress coefficient of the direct tunneling current at very small biases is different from that of the indirect tunneling current. We cannot explain, however, the remaining part of the structure.

The pressure coefficient of sample 1 in the indirect tunneling range is due to the change of the indirect band gap $E_g(111)$ and that of the reduced mass m^*. Neglecting the minor stress variations of C_i and D one can write from Eq. (2)

$$\frac{\Delta I_i}{I_i} = -\beta \left[\frac{3}{2} \frac{\Delta E_g(111)}{E_g(111)} + \frac{1}{2} \frac{\Delta m^*}{m^*} - \frac{\Delta F}{F} \right] . \qquad (13)$$

One may estimate β from Eq. (13) and the measured $\pi_p = 6 \times 10^{-11}$ cm^2/dyne of sample 1 in the forward bias range. Here again it is difficult to estimate $\Delta m^*/m^*$. The reduced mass m^* in Eq. (13) contains the light hole mass and the component of the (111) valley mass tensor in the field direction. The change of the light hole mass can be estimated from Eq. (12) where

$\frac{1}{E_g(000)} \frac{dE_g(000)}{dp} = 12.4 \times 10^{-12}$ cm^2/dyne. The change of the transverse electron mass, which predominantly determines the component of the electron mass in the field direction, is related to the band gap change at the zone face at [111] which is $\frac{1}{E_g} \frac{dE_g}{dp} = 4 \times 10^{-12}$ cm^2/dyne.[17] Hence $\frac{1}{m^*} \frac{dm^*}{dp} = (8 \pm 5) \times 10^{-12}$ cm^2/dyne may be a reasonable estimate. Using this value and the measured pressure coefficient one obtains $\beta = 16 \pm 3$ for V = +60 mV. The same calculation yields the value $\beta = 20 \pm 4$ for V = -70 mV. This increase of β with decreasing bias voltage disagrees strongly with Eqs. (2) and (3) which predict instead a slight decrease of β.[18]

One may think that this discrepancy is due to some simplifying assumptions on which the derivation of Eqs. (2) and (3) is based, in particular the assumptions of (i) a constant junction field, (ii) a parabolic shape of the energy bands in k-space, and (iii) an abrupt transition from n-type to p-type doping. Nathan,[19] however, has calculated the tunneling exponent β using the more realistic field of a graded junction and including non-parabolic effects. He finds that both the variation of the field with position in the junction and a graded impurity distribution, cause β to decrease with decreasing bias voltage even faster than predicted by Eqs. (2) and (3) and that the nonparabolic effects do not influence the bias dependence of β appreciably. In addition

to this Nathan finds that for interpreting the current-voltage characteristic of germanium diodes at 297°K one requires β to decrease with decreasing voltage. In comparing the current-voltage characteristic of the direct tunneling process beyond the Kane kink with Eqs. (2) and (3) in Fig. 5 we also concluded that α decreases with decreasing bias.

In view of this evidence it is difficult to understand the increase of β with decreasing bias voltage as observed in the hydrostatic pressure experiments.

Since one is dealing with the same diode one should be able to calculate β from the previously determined $\alpha = 17.6$ at $V = -300$ mV. Using Eqs. (1), (2), and Kane's value $\lambda_1/\lambda_d = \frac{16}{3\pi}$ one obtains for our case $\beta/\alpha = 1.5$ and hence $\beta = 26.5$ at $V = -300$ mV. This value of β compares well with $\beta = 23.5 \pm 5$ obtained by extrapolating the <u>observed</u> bias dependence of β to $V = -300$ mV. However, in view of the unexpected bias dependence of β, this agreement may be fortuitous.

The contribution to the stress coefficient of sample 2 which arises from the non-equivalence of the two pairs of valleys consists of two parts. (1) The shear causes some electrons to transfer from the two valleys which are raised in energy into the two which are lowered. Those which are lowered are the easy valleys, i.e. they have the smaller m^* in the tunneling direction.

Hence we expect this part to give a positive contribution to π. (2) The shift of the valleys will change also the tunneling probability because the energy gap for a particular valley is changed. Since the easy valleys are lowered in energy, their energy gap decreases under shear. This again results in a positive contribution to π.

Since the first effect involves the density of states factor D one has to write the current as a sum over the j valley contributions and the k phonon contributions

$$I = \sum_{jk} I_{jk} \tag{14}$$

where

$$I_{jk} = A_k \, D(eV \pm \hbar \omega_k/e) \exp(-\beta_j) \tag{15}$$

with

$$B_j = \lambda_i \, E_g^{3/2}(111) \, m_j^{*1/2}/F \tag{16}$$

The plus and minus signs in Eq. (15) indicate that the phonon voltage $\hbar\omega_k/e$ has to be subtracted from the magnitudes of both the forward and the reverse bias voltage for calculating D_k. The coefficients A_k take into account the different electron-phonon interaction strengths for the two phonons.[12] From Fig. 3 we determined $A_2/A_1 = 2.23$ where A_2 refers to the higher energy phonon.

The stress coefficient due to the non-equivalence of the valleys will then be

$$\Delta I/IX = \sum_{jk} \Delta I_{jk} / \sum_{jk} I_{jk} \, X \tag{17}$$

From Eq. (15) one obtains:

$$\Delta I_{jk} = A_k \exp(-\beta_j)\left[\frac{dD_k}{d(\zeta_n)}(\Delta\zeta_n)_j - \frac{3}{2}\frac{D_k\beta_j}{E_g(111)}\Delta E_{g_j}(111)\right] \qquad (18)$$

Since we consider in (17) the pure shear part of the stress only we have

$$\sum_j(\Delta\zeta_n)_j = 0 \quad , \qquad \sum_j \Delta E_{g_j}(111) = 0 \qquad (19)$$

and hence

$$(\Delta\zeta_n)_j = -\Delta E_{g_j}(111) \ . \qquad (20)$$

For uniaxial compression along $[1\bar{1}0]$ one finds

$$\Delta E_{g_3}(111) = -\Delta E_{g_1}(111) = \frac{1}{6} E_2 S_{44} X \qquad (21)$$

Here the subscript 1 refers to the easy valleys j = 1, 2 and subscript 3 to the hard valleys j = 3, 4. E_2 = 19 eV is the deformation potential for pure shear[20] and $S_{44} = 1.47 \times 10^{-12}$ cm^2/dyne is the elastic compliance constant.[21]

In the second term of Eq. (18), which is due to the change in tunneling probability, we have neglected the shear-induced change of the valley masses. Since the reduced mass is determined more by the light hole mass than by the electron mass, this effect is not large. Any change in the light hole mass, however, will affect both samples in the same way and hence will not contribute to the difference of π of the two samples.

Because of the uncertainties involved in the previous determinations of α and β, we have adjusted the value of β_1 so that the magnitude of Eq. (17) agrees with the difference in π of the two samples in the region where only the first phonon contributes. With $\beta_1/\beta_3 = (m^*_1/m^*_3)^{1/2}$ we obtained $\beta_1 = 16$ and $\beta_3 = 18$, both values quoted for V = 0.

Figure 7 shows the comparison of Eq. (17) with the difference in π of the two samples. Although the structure of the bias dependence is reproduced quite well by the theoretical curve, the agreement is only qualitative. The effect of the shift in valley population can clearly be seen in the region between .008 and .030 volts bias. The discrepancy becomes large, however, as soon as the higher energy phonon starts to contribute to the tunneling current. Here the experimental data falls off abruptly from the theoretical curve. There is no known reason why the two phonons should behave differently, but in order to see what would happen, a curve was plotted as though the valleys were equivalent for tunneling involving the higher energy phonons. This curve is shown dashed in Fig. 7. As can be seen from the forward bias data, this modification is too drastic. The data in the reverse bias direction is in better agreement, but it is hard to imagine any mechanism which would distinguish forward from reverse bias. The fall-off of the data in the reverse bias

direction will be affected by exactly the same smearing out mechanisms which are active beyond the Kane kink. If these mechanisms are indeed responsible for the slow fall-off in that region, similar behavior in this bias region is to be expected also. This smearing would not, however, account for the fact that the observed difference between the π of the two samples near V = -0.13 volts is appreciably smaller than the calculated shear coefficient. We therefore conclude that the variation of the inherent tunneling probability per electron is not as sensitive to shear as would be expected. Within the framework of the theory the only possibilities which can account for this are: (a) that the chosen value for β is too low; (b) that the effect of shear on the reduced effective mass is quite large and in the opposite direction as the effect of the valley energy shifts.

There is no value of β which is simultaneously consistent with the shear data and the hydrostatic pressure data. In view of the general agreement between the various independent calculations of β, possibility (a) is unlikely. Possibility (b) can be eliminated also because of the similarity of π for sample 1 and π_p. Furthermore, the mechanism responsible for the discrepancy beyond 30 mV in the forward bias region is undoubtedly also operating in this bias region. It therefore seems that a different mechanism not accounted for by the present theory contributes to the shear stress coefficient.

3. Comparison of Absolute Magnitudes of Tunneling Parameters with Theory

The physical properties of a diode determine the stress coefficients through the parameters α and β. These parameters could not be determined unambiguously from the stress coefficients because the stress-induced changes of the relevant effective masses are not known. These measurements would yield these effective mass changes if it were possible to determine the parameters α and β by some other method. The theory leading to Eqs. (1) and (2) does not determine these parameters accurately enough since it is based on the assumption of a constant junction field and neglects the spatial distribution and fluctuations of the impurity concentrations near the junction.

It is nevertheless interesting to compare and evaluate the values of α and β predicted by the constant junction field theory with the values obtained above from the stress coefficients using reasonable estimates for $\Delta m^*/m^*$. The coefficients α and β can be obtained from the theory, (i) by direct computation using Eqs. (1), (2), and (3), and (ii) by calculating C and D and using the measured I for a given bias voltage. This was done with the following choice of parameters appropriate for our diodes, $\zeta_p = 0.15$ eV, $\zeta_n = 0.020$ eV, $p = 6 \times 10^{19}$, $n = 5.5 \times 10^{18}$, junction area $= 0.002$ cm^2, $\kappa = 16$, $I_d = 0.370$ A at $V = -300$ mV.

The values for α and β obtained by method (i) are listed in the first row of Table I. The third row gives α as calculated by method (ii). The value of β could not be obtained in this way because the electron phonon coupling constants are not known. The fourth and fifth rows list the values obtained from the experimentally observed hydrostatic pressure coefficients as explained in the previous section. The last row gives the value of β used to fit the shear contribution to the stress coefficient of sample 2 in the bias range of indirect tunneling. The bias voltages at which the listed quantities were obtained are included in Table I.

It is seen that α and β as computed from the constant field expressions Eq. (1), (2), and (3) are appreciably smaller than the other values. This is to be expected since a real diode will have a more diffused distribution of impurities and hence a smaller impurity concentration near the junction than in the bulk material. This yields a wider junction. Following Meyerhofer et. al.[22] we assume the donor concentration near the junction to be half of that of the bulk and obtain by direct computation of α and β the values quoted in the second row of Table I.[23]

The uncertainty of the experimental values stems from the difficulty of estimating $\Delta m^*/m^*$ and also from the fact that for the pressure coefficients of the energy gaps the values measured on pure material at $300^{\circ}K$ were used. It is hoped to obtain the

temperature dependence of these pressure coefficients by studying the stress tunneling coefficients at elevated temperatures.

V. SUMMARY AND CONCLUSION

The magnitude and the orientation dependence of the effect of stress on the tunneling current enables one to distinguish three different tunneling processes in Sb-doped germanium.

(1) In the small bias range -8 mV < V < +8 mV the tunneling is direct. The detailed nature of the tunneling process in this range is not known. The current is not affected by the relative shifts of the (111) valleys under shear and hence cannot arise from a sum of independent (111) valley contributions.

(2) Beyond about 8 mV at helium temperatures, but before the onset of direct tunneling into the (000) conduction band, the tunneling process is phonon assisted. Here a large additional contribution to the stress coefficient is observed for a shear stress which lifts the degeneracy of the (111) valleys when the orientation of the junction field is such that the effective mass components of the valleys in the field direction are different. This demonstrates clearly the anisotropy of the tunneling probability when the effective mass is anisotropic as predicted by the theory.

(3) For biases V < -140 mV direct tunneling into the (000) conduction band is observed. Near the onset voltage V_k the magnitude of the stress coefficients increases sharply because

of the pressure dependence of V_k. This sharp increase allows an accurate determination of $E_g(000) - E_g(111)$, the energy separation between the conduction band edges at (000) and (111), respectively. We find for this the value 0.160 ± 0.005 eV which is about 0.015 eV larger than that for pure material. This larger value of the conduction band separation agrees with recent results of infrared absorption measurements[16] in degenerate germanium. The sharp rise of the stress coefficients near $V = V_k$ indicates that the (000) conduction band edge is quite well defined despite the large impurity concentration.

The major features of the bias and orientation dependencies of the stress coefficients agree with the present theory of tunneling. There are, however, several interesting observations which remain unexplained at present. One is the structure in the bias dependence of the pressure coefficient π_p. The magnitude of π_p changes near $V = \pm 8$ mV and $V = \pm 30$ mV. These voltages agree closely with the onsets of the TA and the LA phonon contributions. The second is the disagreement between the theoretically predicted shear contribution to π with the experiments in the bias range where LA phonons can be emitted. The third observation which needs some further study is the bias dependence of the indirect tunneling exponent β which is found to be opposite to the prediction of theory.

ACKNOWLEDGMENTS

It is a pleasure to acknowledge the able help of G. Rochlin who took the measurements. We are also pleased to acknowledge the general support of the Low Temperature Laboratory of the University of Chicago by the National Science Foundation and by the U.S. Atomic Energy Commission which made this work possible.

HF:JJT:erm
11/28/62

TABLE I

Values of Tunneling Exponents α and β

	α	Bias (mV)	β	Bias (mV)
Theory	8.5	-300	12.5	-300
Theory (see text)	12	-300	17.5	-300
Theory and I_d	12.5 ± 1	-300		
Pressure Exp.	17.6	-300	16 ± 3	+ 60
Pressure Exp.			20 ± 4	- 70
Shear Exp.			17 ± 1	0

REFERENCES

1. L. Esaki, Phys. Rev. 109, 603 (1958).
2. L. V. Keldysh, Soviet Phys. JETP 6, 763 (1958); 7, 665 (1958); W. Franz, Z. Naturf. 14a, 415 (1959); E. O. Kane, J. Phys. Chem. Solids 12, 181 (1959); P. J. Price and J. M. Radcliffe, IBM Journal 3, 364 (1959); W. P. Dumke, P. B. Miller and R. R. Haering, J. Phys. Chem. Solids 23, 501 (1962).
3. E. O. Kane, J. Appl. Phys. 32, 83 (1961).
4. R. W. Keyes, in Solid State Physics edited by F. Seitz and D. Turnbull (Academic Press, Inc., New York, 1960), Vol. II, p. 149.
5. N. Holonyak, I. A. Lesk, R. N. Hall, J. J. Tiemann, and H. Ehrenreich, Phys. Rev. Ltrs. 3, 167 (1959); Y. Furukawa, J. Phys. Soc. Japan 15, 1903 (1960); R. N. Hall, Proc. Int. Conf. Semiconductor Physics, Prague 1960, p. 193.
6. J. V. Morgan and E. O. Kane, Phys. Rev. Ltrs. 3, 466 (1959).
7. R. N. Hall and J. H. Racette, J. Appl. Phys. 32, 2078 (1961).
8. W. Paul, J. Phys. Chem. Solids 8, 196 (1959).
9. C. Herring and E. Vogt, Phys. Rev. 101, 944 (1956).
10. The tunneling direction for isotropic effective masses is along the direction of the electric field (perpendicular to the plane of the junction). For an anisotropic effective mass, the tunneling direction lies between the electric

field direction and the direction of minimum effective mass. We have assumed that in all cases the tunneling direction coincides with the electric field; so we have slightly overestimated the non-equivalence of the valleys.

11. There is another mechanism by which shear can produce a first order effect. In addition to a change in the valley energy, shear causes a deformation of the effective mass ellipsoids. Since tunneling depends only on the projection of the effective mass along the direction of tunneling, rather than an average over all directions, a linear effect occurs. This effect operates even when the valley in question is at a point of symmetry such that the valley energy cannot depend on shear.

12. There is additional structure due to the optical phonons. Since this structure is small, we have treated the contribution of these phonons together with that of the higher energy acoustic phonon.

13. These impurity cell potentials give rise also to the valley-orbit splittings of the 1s-like states of isolated Group V donor impurities in Ge and Si.

14. E. O. Kane, J. Phys. Chem. Solids 7, 249 (1957). For the relationship between effective masses and energy gap see also H. Ehrenreich, J. Appl. Phys. 32, 2155 (1961).

15. G. G. Macfarlane, T. P. McLean, J. E. Quarrington, and V. Roberts, Proc. Phys. Soc. 71, 863 (1958).

16. C. Haas, Phys. Rev. 125, 1965 (1962).

17. H. R. Philipp, W. C. Dash, and H. Ehrenreich, Phys. Rev. 127, 762 (1962).

18. This effect was also observed by M. I. Nathan and W. Paul (Proc. Int. Conf. Semiconductor Physics, Prague 1960, p. 209).

19. M. I. Nathan, J. Appl. Phys. 33, 1460 (1962).

20. H. Fritzsche, Phys. Rev. 115, 336 (1959).

21. M. E. Fine, J. Appl. Phys. 24, 388 (1953).

22. D. Meyerhofer, G. A. Brown, and H. S. Sommers, Phys. Rev. 126, 1329 (1962).

23. Nathan discussed and employed a method for obtaining β from the bias dependence of the reverse current at room temperature (see reference 19). Although several aspects of the shape of the I-V characteristic still remain unexplained we have used his method and find for our samples at zero bias $\beta = 18 \pm 1$ using his best fit parameter $\gamma = 1.25$.

FIGURE CAPTIONS

Fig. 1 Stress coefficients for uniaxial [1$\bar{1}$0] compression and hydrostatic pressure as a function of bias voltage at 4.2°K.

Fig. 2 Current-voltage characteristic of one diode of sample 2 at 4.2°K. Note the onsets of the TA and LA phonon contributions near the bias voltages $\pm$ 8 mV and $\pm$ 28 mV, respectively.

Fig. 3 Current as a function of reverse bias of one diode of sample 2 at 4.2°K. Note the sharp increase in current near V = -140 mV.

Fig. 4 Relative position of the bands and Fermi levels in a germanium tunnel diode for a reverse bias beyond the Kane kink.

Fig. 5 Comparison between theory and experiment of the bias dependence of the direct tunnel current beyond the Kane kink. The factor C_d of Eq. (1) (see text) has been chosen to fit the absolute magnitude of the theoretical and experimental I_d near -220 mV reverse bias.

Fig. 6 Comparison between theoretical and experimental stress coefficient for reverse bias voltages beyond the Kane kink.

Fig. 7 The difference between the uniaxial stress coefficients of samples 1 and 2. Comparison between theory and

experiment. The heavy curve represents the theory based on the anisotropy of the tunneling probability in the whole bias range of indirect tunneling. The dotted curve was calculated assuming that the (111) valleys are equivalent for tunneling involving the higher energy phonon.

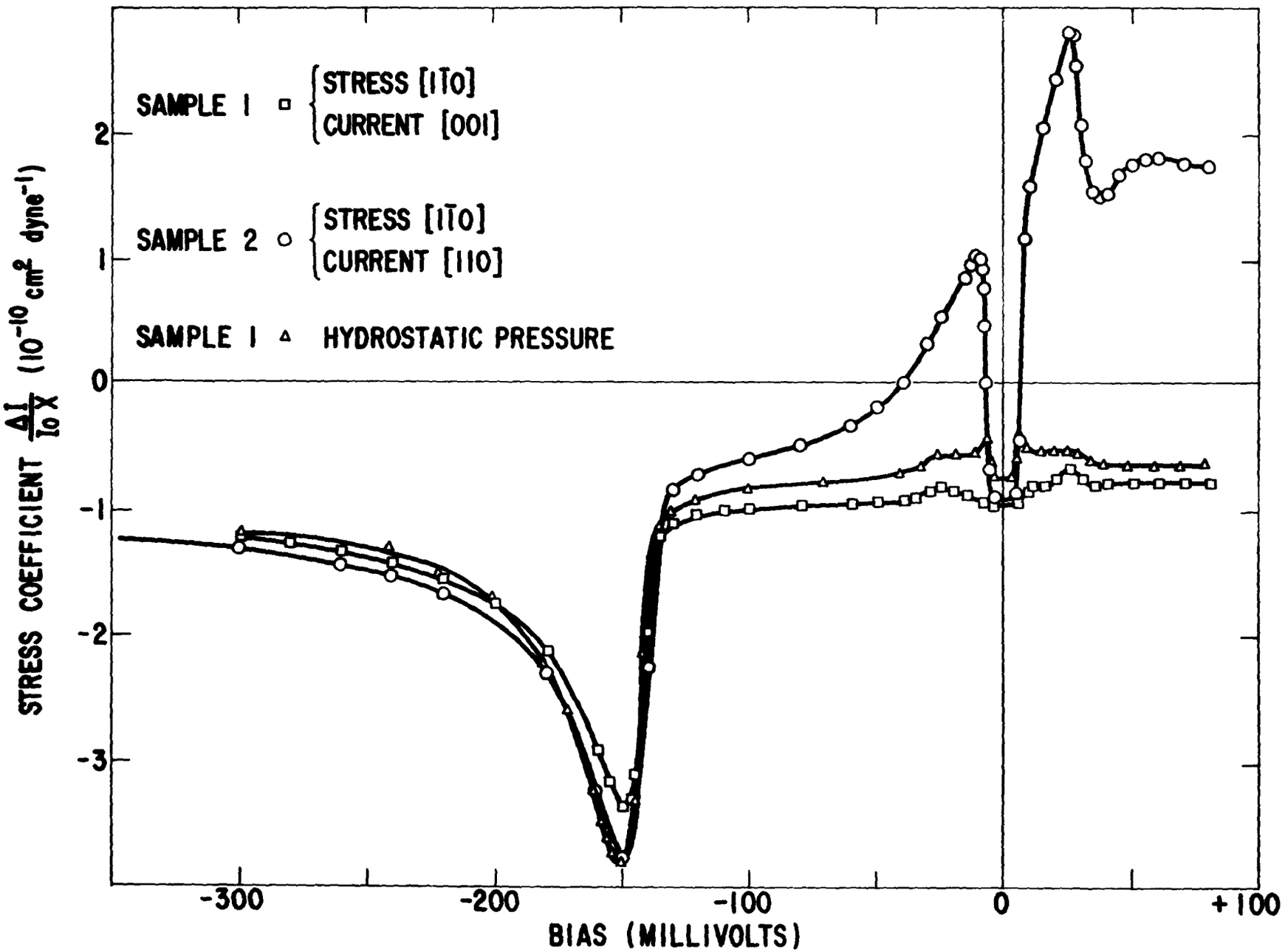
SAMPLE 1 □ STRESS [1$\bar{1}$0] CURRENT [001]
SAMPLE 2 ○ STRESS [1$\bar{1}$0] CURRENT [110]
SAMPLE 1 △ HYDROSTATIC PRESSURE
STRESS COEFFICIENT $\frac{\Delta I}{I_0 X}$ (10^{-10} cm^2 dyne^{-1})
2
1
0
-1
-2
-3
-300
-200
-100
0
+100
BIAS (MILLIVOLTS)

Fig. 1

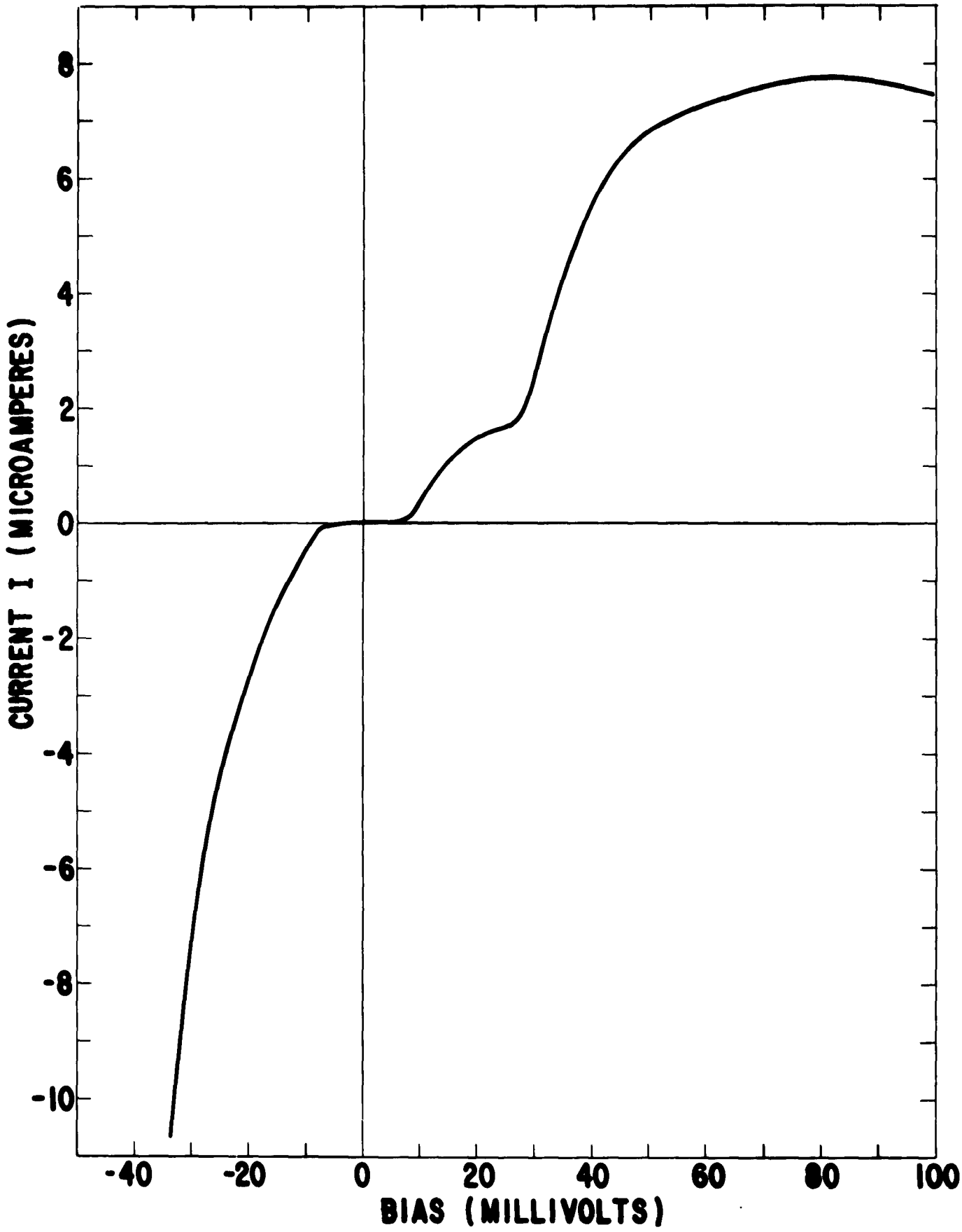
8
6
4
2
0
-2
-4
-6
-8
-10
CURRENT I (MICROAMPERES)
-40
-20
0
20
40
60
80
100
BIAS (MILLIVOLTS)

Fig. 2

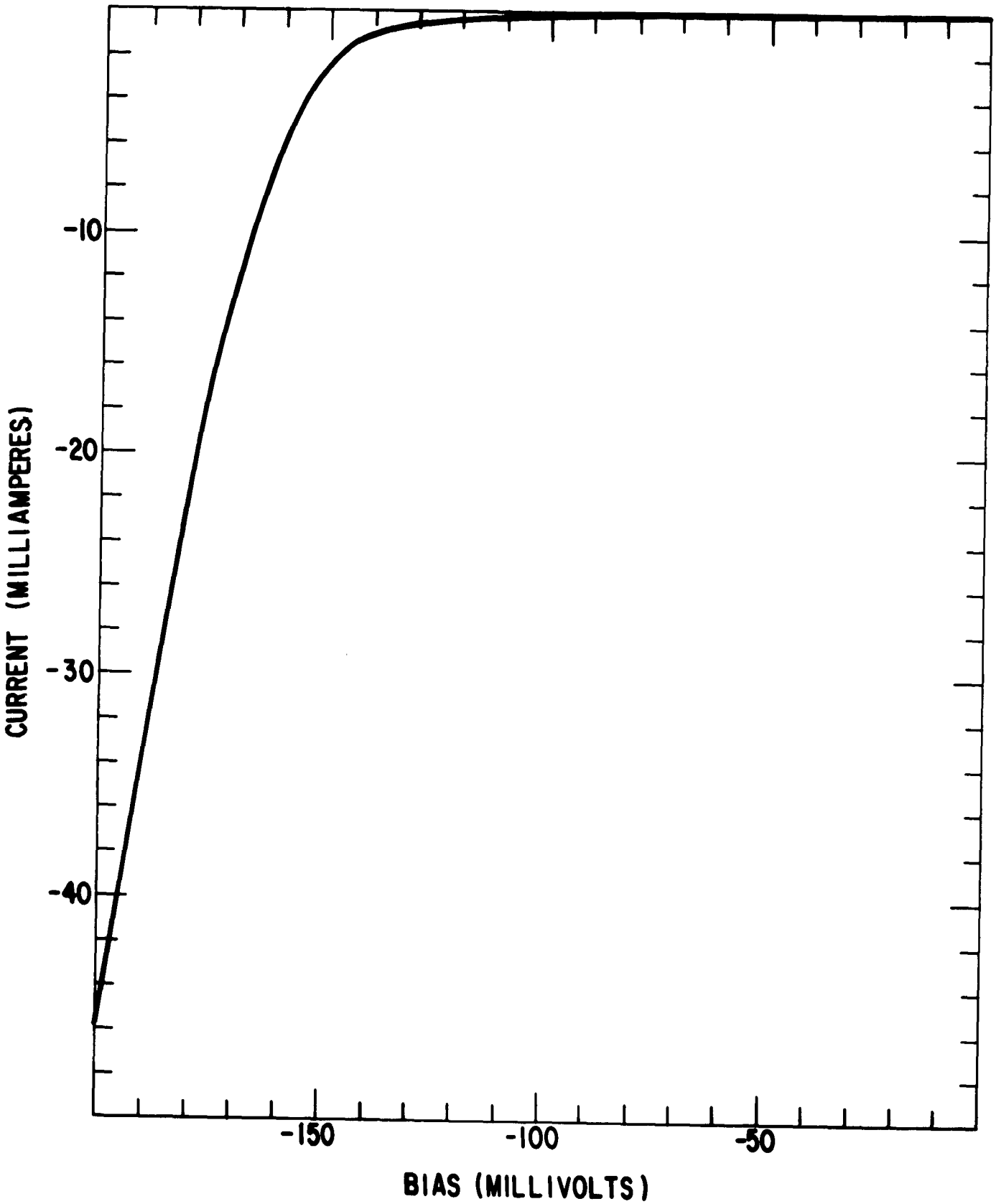

Fig. 3

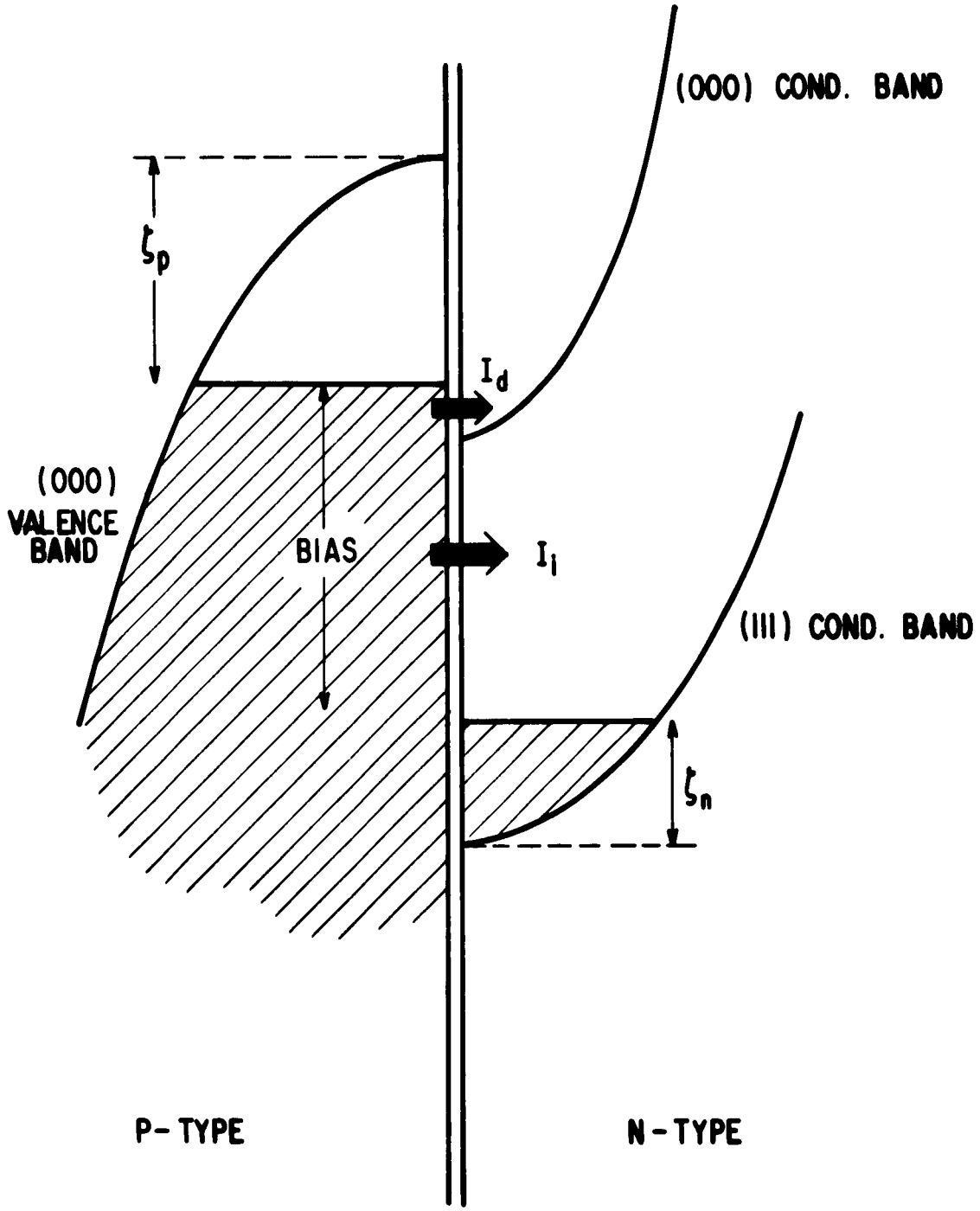
(000) COND. BAND
ζ_p
I_d
(000)
VALENCE
BAND
BIAS
I_i
(111) COND. BAND
ζ_n
P-TYPE
N-TYPE

Fig. 4

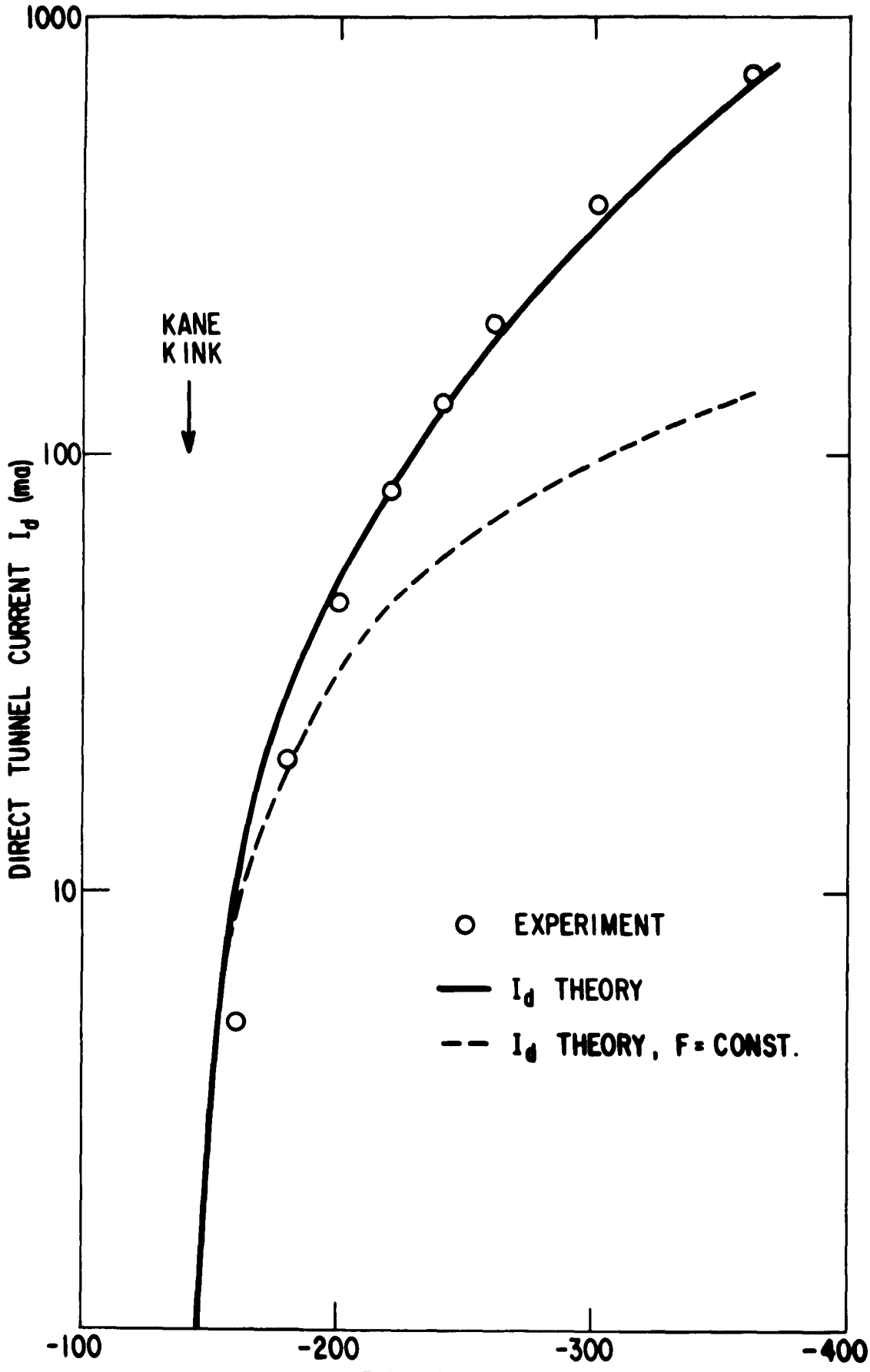
1000
100
10
KANE
KINK
DIRECT TUNNEL CURRENT I_d (ma)
EXPERIMENT
I_d THEORY
I_d THEORY, F = CONST.
-100
-200
-300
-400
BIAS (MILLIVOLTS)

Fig.5

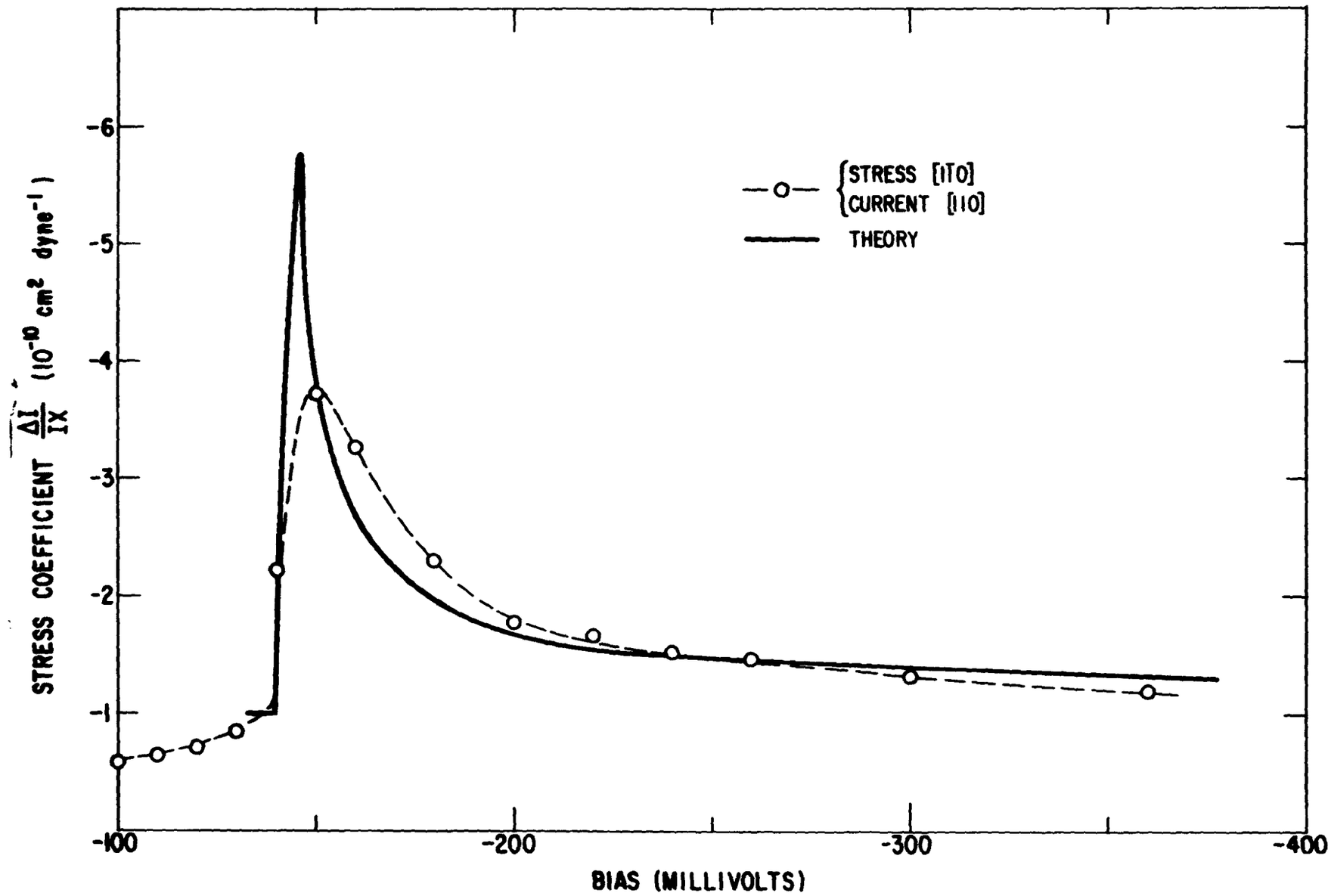
STRESS [1T0]
CURRENT [110]
THEORY
STRESS COEFFICIENT $\frac{\Delta I}{IX}$ (10^{-10} cm^2 dyne^{-1})
-6
-5
-4
-3
-2
-1
-100
-200
-300
-400
BIAS (MILLIVOLTS)

Fig.6

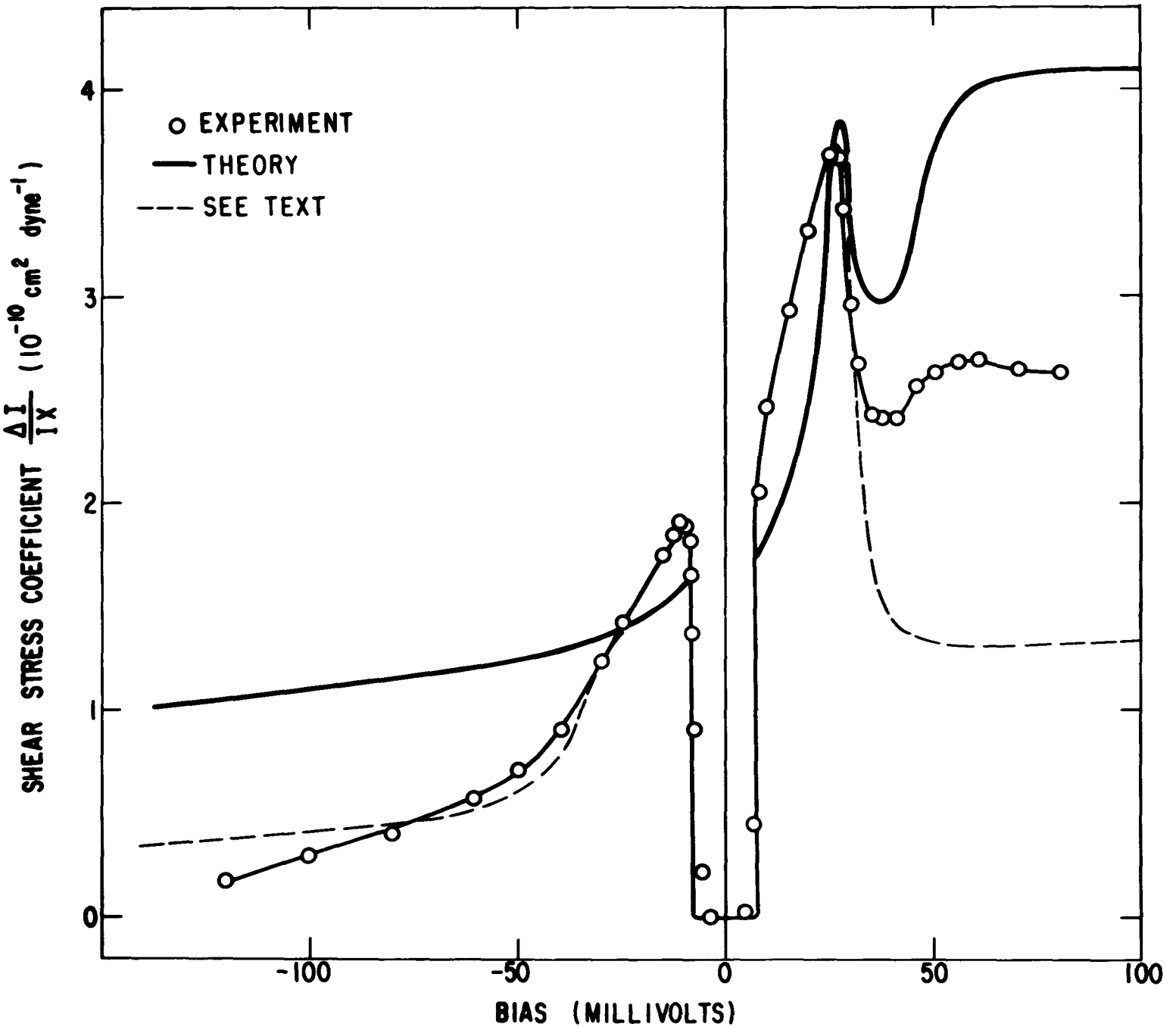
EXPERIMENT
THEORY
SEE TEXT
SHEAR STRESS COEFFICIENT $\frac{\Delta I}{I X}$ (10^{-10} cm^2 dyne^{-1})
4
3
2
1
0
-100
-50
0
50
100
BIAS (MILLIVOLTS)

Fig. 7

B. Carrier Mobility and Shallow Impurity States in ZnSe and ZnTe

(M. Aven and B. Segall)

I. INTRODUCTION

Several of the II-VI compounds have been under investigation by luminescence and photoconductive techniques for a great many years. Much of this work was directed toward the goal of understanding the role of the impurities and of identifying the states associated with them. Despite this work, however, the identification of the specific impurity states is still a matter of considerable debate and uncertainty. At present there is still little conclusive evidence about the identity of any shallow impuritystates, which, for example, play an important role in the optical properties of these crystals.

The primary aim of the present work was to obtain information about the shallow donor and acceptor levels in some of the II-VI compounds by means of electrical transport studies. In the past extensive electrical measurements have not generally been possible due to the unavailability of suitable material. However, considerable advances have recently been made in the preparation of some of these materials, including the compounds that are the subject of the present study, ZnSe and ZnTe.[1,2,3] It is, of course, well known that in addition to yielding information about the energy levels of the defects, the electrical transport measurements provide

a valuable means for studying the mechanism by which the carriers are scattered. This question was considered in some detail for the two compounds studied.

In earlier work, the results of optical and preliminary electrical measurements on ZnSe were reported.[4,5] The electrical measurements of the n-type material have been extended in the present work. Besides the previously described material with 0.19 ev deep donor levels,[5,6] and the more strongly n-type material containing donors with ionization energies of 0.01 eV,[5] it has now been possible to prepare ZnSe exhibiting degenerate conduction characteristics.

We have also extended the investigation of the transport properties of p-type ZnTe. The study of this compound is of considerable interest since the knowledge gained about the transport of holes in the valence bands and of the acceptor states would be expected to be helpful in understanding the corresponding properties and states of the other II-VI semiconductors. In regard to the study of acceptor levels, significant progress was made possible as a result of the successful purification by the zinc extraction technique recently described by Aven and Woodbury.[7] By impurity diffusion and extraction cycles, in conjunction with radioactive tracer studies, it was possible to identify the acceptor levels associated with the most prominent acceptor impurities--Cu, Ag,

and Au. Concomitantly, the acceptor state of the native defect, which we believe to be the zinc vacancy, could be identified. It is to be emphasized that analogous states are believed to be associated with the other crystals of this family of semiconductors, but until this time the identification of these states has not been conclusively established.

From the study of the Hall mobility, the intrinsic (or lattice) mobility for the two materials could be determined for temperatures above about 100°K. The various possible lattice scattering mechanisms were considered with the aim of determining which of them play the major role in limiting the intrinsic mobility. For n-type ZnSe it is found that the electrons are scattered much more strongly by the polar scattering of optical phonons than by other mechanisms. A similar conclusion is probably also true for ZnTe, unless the parameter characterizing the strength of the non-polar coupling to the optical mode phonons is much larger than presently believed.

II. EXPERIMENTAL

The ZnSe and ZnTe crystals were grown by the vapor growth technique first described by Greene et al[8] and modified by Piper and Polich.[9] The starting material for ZnSe was General Electric Chemical Products Plant ZnSe powder which was first sintered in the presence of excess Se in hydrogen atmosphere. ZnTe was

synthesized by heating together high purity Zn obtained from the Consolidated Mining and Smelting Co. and high purity Te obtained from the American Smelting and Refining Co. The single crystals were grown by passing the sintered charge at the rate of approximately 0.2 mm/hr through a furnace heated to 1350°C for ZnSe and to 1050°C for ZnTe. The product was usually a boule of several cm^3 containing single crystal regions of a tenth to one cm^3.

The majority of the crystals were subjected to the purification technique in which the crystals are heated in contact with molten Zn at 900-1000°C for one or two days. This treatment has been shown[7] (by using radioactive tracer techniques) to reduce the concentration of the acceptor impurities Cu and Ag in II-VI compounds to the 10^{14} to 10^{15} cm^{-3} range. With the exception of Cl-doped ZnSe, all the doped crystals were obtained by diffusing impurities into crystal purified by the solvent extraction method. Chlorine-doped ZnSe was prepared by adding $SrCl_2$ to the starting material prior to the crystal growth.

The Hall measurements were performed with sample bars 8-10 mm long and 1-4 mm^2 in cross sectional area, cut from the boules described above. Prior to electroding the bars were chemically polished in hot concentrated NaOH. The electrodes to ZnSe were In dots fused in under hydrogen atmosphere at 300°C. The electrodes to ZnTe were chemically formed Au patches, to which Pt wires were soldered with In-Ag alloy.

The Hall effect apparatus used for electrical measurements covered the range from liquid hydrogen temperature to approximately 150°C. The measurements were performed by the standard six electrode technique widely used on semiconductor materials. The voltage drop across the crystal was usually of the order of 0.1 V. The magnetic fields used were between 7 and 8 kgauss. To assure that no irreversible changes had occurred in the bulk of the crystals or the electrodes during the thermal cycling, several of the crystals were remeasured over the entire covered temperature range. A few crystals were removed from the apparatus, re-electroded and remeasured. In no cases were any irreversible effects observed. However, with all crystals a minimum temperature was always encountered below which the measurements became unreliable because of the onset of non-ohmic behavior of the electrical contacts. Thus for any given crystal the temperature range for which the measurements are given was determined by the lowest temperature at which the Hall voltage and the potential drop across the crystal were linear functions of the current through the crystal.

III. RESULTS AND DISCUSSION

Before discussing and analyzing the experimental results, it is useful to state the assumptions about the band structure of ZnSe and ZnTe that will be used. It appears that both of these compounds are direct transition semiconductors, presumably having the absolute extrema of their conduction and valence bands at $k = 0$.

These conclusions are based primarily on the absorption spectra[4,10] (particularly on the sharp exciton lines which are not appreciably broadened by autoionization) and on the emission spectra[11,12] which exhibit sharp lines very close to the band edges.[13] Since we will only be concerned with n-type ZnSe and p-type ZnTe, only the assumptions about the location of the conduction band minimum of the former and the valence band maximum of the latter will have a bearing on the following discussion. The chief effect of this assumption will be to exclude the possibility of intervalley scattering.

In addition, it will be necessary to assume values for the effective masses for the carriers. On the basis of a reduced exciton mass of $(0.10 \pm .03)$ m as deduced in the optical studies of ZnSe[4], we take $m^* = 0.15$ m as a reasonable estimate of the electron mass. Since information relating to the hole mass in ZnTe is unavailable, we are forced to make a more arbitrary choice in this case based on the known hole masses in CdS[14] and CdSe.[15] We take the value of 0.6 m for the density of states mass. Inasmuch as we are not seeking to precisely fit the data, this estimate of the hole mass should be adequate for our purpose.

In analyzing the carrier concentration data from a single level, we will use the well-known formula[16] for non-degenerate statistics, e.g.

$$\frac{p(p + N_d)}{(N_a - N_d - p)} = \frac{N_v}{g} \exp(-E_a/kT) \qquad (1)$$

for the hole concentration p. Here $N_v = 2(2\pi m_v kTh^{-2})^{3/2}$, m_v being the density of states mass and g the degeneracy factor which depends on the nature of the impurity state and the band edge involved. Later when considering the carrier concentration associated with an imperfection which we believe to be a double acceptor, we will set up the generalization of (1) appropriate to that case. In the following, we will take the carrier concentrations p and n to be given by $|R_H e|^{-1}$ for simplicity, where R_H is the Hall constant and e the electronic charge. The factor $r = \mu_H/\mu_d$,[16] the ratio of Hall to drift mobilities is thus taken to be unity. This is, in fact, a fairly good approximation since r is reasonably close to unity for polar scattering[17] which we will show below to be the principal scattering mechanism in the temperature range of primary interest here.

1. ZnTe - Impurity and Native Defect Levels

In the following we will discuss the results of Hall measurements on several ZnTe crystals prepared in such a way as to produce a dominance of one type of impurity (including native defect) over all others. With such crystals it is a straightforward matter to identify the various defects giving rise to the energy levels found by the electrical measurements.

A survey of the behavior of the Hall constant R_H vs. T^{-1} for typical undoped crystals and crystals doped with the noble metals

is provided by Fig. 1. From the curve for the undoped sample, the p-type nature of which we believe to be due to a Zn vacancy, an ionization energy of 0.048 eV is found. The acceptor ionization energies for the Cu, Ag, and Au-doped samples are found to be 0.15 eV, 0.11 eV, and 0.22 eV respectively.

Figure 2 shows more detailed data for a crystal which was found by chemical analysis to contain Cu at a concentration of $(2 \pm 1) \times 10^{16}$ cm^{-3}. The behavior at low T corresponds to the freeze-out of the holes into an acceptor level at 0.15 eV as in the Cu curve of Fig. 1. Using the value of g = 4 which is appropriate for a simple acceptor associated with the four-fold degenerate valence band maximum[18] it is possible to satisfactorily fit the data with $N_A = 3.4 \times 10^{16}$ cm^{-3} and $N_D = 3.1 \times 10^{15}$ cm^{-3}. In Fig. 2 the experimental points are indicated by circles, and the theoretical values by the solid curve. It should be noted that the above value of N_A agrees reasonably well with the result of the chemical analysis.

Figure 3 shows the free hole concentration vs T^{-1} for four undoped ZnTe crystals fired under different Te pressures. The shapes of these curves are sufficiently similar to indicate that the same level is involved in all the crystals. The energy value that corresponds to the low temperature end of the curves is 0.048 eV (the temperature range for the two lower curves being admittedly very small). The vertical displacement of these curves

from one another indicates that the free hole concentration at any temperature increases with increasing partial pressure of Te. The increasing partial pressure of Te increases the concentration of Zn vacancies, which in turn increases the free hole concentration. These results are consistent with our belief that the native acceptor center is the Zn vacancy.

The above evidence per se does not preclude the possibility that the acceptor is interstitial Te. However, this possibility can probably be ruled out on the basis of the very large size of the Te atom and also because it appears unlikely that interstitial Te could bind extra electrons. The tendency of ZnTe to form an excess of Zn over Te vacancies, on the other hand, is consistent with the greater volatility of Zn.

The Zn vacancy is expected to be a double acceptor. In contrast to the curves for the Cu, Ag, and Au-doped samples, the curves for the undoped samples have a shape above about 200°K which suggests the ionization of holes from a deeper level. In order to check the identification and determine the ionization energy of the deeper level, it would be desirable to have hole concentration data available over a wide high temperature range, and to fit these data with the expression for p appropriate to the case of a double acceptor associated with the fourfold degenerate valence band. Although the present data is perhaps not as extensive as would be desired, it still is useful for a

preliminary investigation of this point. To obtain the equation for p we use for the probabilities that the double acceptor is in the neutral, single, or doubly ionized state the expressions derived by Teitler and Wallis,[18] which are

$$N_a^{o}/N_a = 6\, R_o^{-1} \left\{ \exp[2\alpha + \beta(E_1 + E_2)] \right\}$$

$$N_a^{-}/N_a = 4\, R_o^{-1} \exp[\alpha + \beta E_2] \qquad (2)$$

$$N_a^{2-}/N_a = R_o^{-1}$$

with $N_a^{o} + N_a^{-} + N_a^{2-} = N_a$, $\alpha = -E_F/kT$, and $\beta = 1/kT$. For non-degenerate statistics, the charge neutrality condition $p + N_d = N_a^{-} + 2N_a^{2-}$ leads to the following cubic equation for p:

$$6p^3 + p^2 [4N_v^{(1)} + 6N_d] + p [N_v^{(1)} N_v^{(2)} + 4N_v^{(1)} (N_d - N_a)]$$

$$+ N_v^{(1)} N_v^{(2)} (N_d - 2N_a) = 0 \qquad (3)$$

where $N_v^{(i)} = N_v \exp(-E_i/KT)$ for i = 1 and 2. At temperatures low enough so that $N_v^{(2)}$ is negligible Eq. (3) reduces to Eq. (1) with g = 3/2 which is the correct statistical factor[19] for this case, while at high temperatures it leads to the proper saturation value of $2N_a - N_d$.

The solid curves in Fig. 3 represent the fit of the data for the three lower Te pressures using Eq. (3). The sample fired at the highest Te pressure was only fitted at low temperatures, using

Eq. (1), as this sample was not purified by the Zn extraction method and was known to contain some Cu.[20] In Eq. (3) we used the previously determined value of 0.048 eV for E_1, and 0.13 eV for E_2, although a range of values (roughly 0.12 to 0.16 eV) for E_2 provided reasonably good agreement. The acceptor concentrations, N_a, determined from the fitting of the data for the samples fired under the Te pressures of 10^{-6}, 0.04 and 0.15 atm., were approximately 0.35×10^{17}, 1.2×10^{17} and 1.7×10^{17} cm^{-3}, respectively. The value of $0.14 \pm .02$ eV for E_2 is admittedly rather close to the ionization energy for Cu acceptors. The high temperature portion of the curves cannot, however, be due to Cu in the purified samples for, as will be shown below, its concentration in these samples is much too low. It is of course possible that the ZnTe crystals contain an unidentified acceptor, unextractable by the liquid Zn treatment, in concentrations comparable to that of the Zn vacancies, and that the observed level is due to it. We believe this possibility to be unlikely.[21] However, before the deeper level can be definitely established as the second charged state of the Zn vacancy, more extensive investigations on additional purified and analyzed samples over a more extended high temperature range would be required.

Three experiments were performed to assure that the thermal treatment to which the crystals were subjected during the diffusion process was not producing other significant changes besides the

incorporation of the desired impurities. First, Cu was diffused into two ZnTe crystals which were previously fired under 2 atm Zn pressure and 0.5 atm Te pressure[22] respectively and which exhibited the 0.048 eV acceptor levels. In each case the incorporation of Cu resulted in the disappearance of the 0.048 eV level and the appearance of the 0.15 eV level.

In a complementary experiment two crystals, previously doped with Cu and exhibiting the 0.15 eV level, were fired in liquid Zn and liquid Te, respectively. In each case the crystals lost their 0.15 eV levels and acquired the 0.048 eV levels. One crystal was subjected to several Cu diffusion-Zn extraction cycles and was found always to come back to the 0.15 eV level after Cu diffusion and to the 0.048 eV level after the Zn extraction. An analogous behavior was observed with an Ag diffusion-Zn extraction cycle and an Au diffusion-Zn extraction cycle.

In the third experiment the radioactive isotopes Cu^{64} and Ag^{110} were separately diffused into two undoped ZnTe crystals. The incorporation of the radioactive dopants was carried out by exactly the same technique as that used with the crystal on which the Hall measurements were performed. The Cu and Ag concentration after the diffusion, as determined by an appropriate counting technique, was approximately 10^{17} cm^{-3}. By several successive etchings and countings it was found that the dopants were uniformly distributed throughout the body of the crystal. After extracting

both crystals with liquid Zn, the residual concentration of Cu and Ag in them was found to be approximately 10^{14} cm^{-3}.

These experiments show that the introduction of the employed acceptor impurities is independent of whether the crystal was previously fired under Zn or Te atmosphere. Because of the reversibility of the impurity diffusion-Zn extraction cycles, it is also certain that electrically active uncontrolled impurities were not entering the crystals in significant amounts during the various firing techniques to which the crystals were subjected. It is significant to note that the analysis of the carrier concentration of the Cu doped sample discussed above leads to an acceptor concentration in fair agreement with the Cu concentration determined by chemical analysis. The experiment with the radioactive Cu and Ag demonstrates that the employed diffusion technique leads to a uniform distribution of the dopant in the crystal in concentrations where it exists in the crystal as the dominant impurity. The complementary study of the removal of the Cu and Ag radioisotopes by Zn extraction shows that the residual concentration of these impurities in the crystals subjected to this purification technique is several orders of magnitude below the concentration of any of the intentionally introduced acceptors which have determined the electrical properties of the crystals.

Thus we see there are acceptor states in ZnTe having ionization energies of 0.15, 0.11, and 0.22 eV definitely associated with the

presence of Cu, Ag, and Au respectively. The simplest interpretation of these results is that these metal impurities go into ZnTe substitutionally replacing the Zn. The acceptor states are then directly attributable to the impurities. One feature of this picture which is perhaps disturbing is the closeness of E_a for Cu and for the second level of the Zn vacancy. This circumstance might suggest the possibility of more complex models for the acceptors. For example, it might be assumed that Cu acts as a donor but that it is paried with the vacancy. The 0.048 eV vacancy level is thereby compensated. While complex models like this cannot be completely excluded at present, their complexity alone makes them less attractive. Unless further evidence is adduced to indicate that complexes are involved, we tend to favor the simpler model of the acceptor. The near equality of the two ionization energies is believed to be fortuitous.

2. ZnSe - Donor Levels

The information to be reported below about donor levels in ZnSe is much less detailed than the above study of acceptor levels in ZnTe. Although the Zn extraction method was found to remove acceptor impurities from ZnSe as effectively as from ZnTe, as yet little is known of its effect on donor impurities. Therefore, in the experiments with n-type ZnSe to be described below, it was not possible to identify the donor levels with particular impurities or native defects.

Figure 4 shows the results of Hall measurements for a ZnSe crystal grown with 10^{19} cm^{-3} Cl (as determined by chemical analysis) and subjected to one extraction with liquid Zn. From the behavior of R_H between 100°K and room temperature, a donor level at 0.19 eV is determined. This value is very close to the 0.21 eV level found by Bube and Lind[6] in Br-doped ZnSe. It is possible that these levels are due to the halogen dopants used, although the identification has yet to be conclusively established.

The previously reported donor ionization energies in ZnS and ZnSe are in the range of 0.2 to 0.3 eV while those for CdTe, CdSe, and CdS are much smaller[6] and are approximately equal to those expected on the basis of the hydrogenic model (i.e. 0.01 to 0.03 eV). The donor depth of ZnSe predicted by the hydrogenic model, $E_d = 13.6\ (m^*/m)\ \epsilon_s^{-2}$ eV, for the estimated m^*/m of 0.15 and for the static dielectric constant ϵ_s of 8.1, is 0.03 eV. This is almost a factor of ten less than the value of about 0.2 eV noted above.

The question arises as to why a shallow level is not found in ZnSe (and also in the other zinc compounds) while shallow levels are found in the cadmium compound semiconductors. A simple explanation of this could be obtained from the fact that the previous observations have been made in insulating or weakly n-type crystals. This suggests that the shallow levels were completely compensated, and therefore did not contribute to the free carrier concentration.

This explanation was tested by preparing a more strongly n-type sample by subjecting an undoped[23] crystal to two successive Zn extractions in an attempt to reduce the concentration of the compensating acceptors. From the data for this sample, shown as the intermediate curve in Fig. 4, it can be seen that the carrier concentration is higher and the slope much lower than for the previous sample. Using Eq. (1) with g = 2, which is appropriate to the case of a simple donor, the data are fitted using N_d = 9.5×10^{16} cm^{-3}, N_a = 8.7×10^{16} cm^{-3} and E_d = 0.008 eV. The calculated points are shown as triangles in Fig. 4. This level is indeed shallow. In fact, it is considerably shallower than the hydrogenic value. At these moderately large values of N_d and N_a, the latter fact undoubtedly reflects the dependence of the ionization energy on impurity concentration as has been observed, for example, in Ge.[24] The relatively large degree of compensation, found to be present in this sample in spite of the extraction of acceptor impurities and the suppression of the concentration of native acceptors (Zn vacancies) by the liquid Zn treatment, demonstrates the strong tendency of ZnSe toward self-compensation.

Finally, a sample with a still higher carrier concentration was prepared by diffusing 1.5×10^{20} cm^{-3} Al into a previously purified ZnSe crystal. The Hall constant for this crystal is given as the lowest curve in Fig. 4. It is evident from the fact that R_H is constant from about 16°K to 370°K that the ionization

energy has vanished. Evidently the impurity concentration is greater than the critical value at which $E_d = 0$, and the Fermi level either coincides with the conduction band edge or lies within the conduction band. The sample thus represents the first case of degenerate conduction in the zinc II-VI compounds.

3. Mobilities of ZnTe and ZnSe

The mobility data for ZnSe and ZnTe are presented in Figs. 5 and 6 respectively. While more extensive data might be desirable for a detailed analysis of the mobilities, the present results are quite adequate to permit a study of the dominant scattering mechanisms. From the near equality of the mobilities (μ) for $T > 100^{\circ}K$ for samples with significantly different defect concentrations and from their fairly rapid increase with decreasing temperature, it appears that the μ for $T > 100^{\circ}K$ are determined by the intrinsic properties of the two materials and not by the crystal defects. In addition it will be shown below that the magnitude and temperature dependence can in fact be accounted for by a lattice scattering mechanism. Below about $100^{\circ}K$ on the other hand, charged impurity scattering is indicated by the increase in μ with temperature. This is supported by the study of μ for the one sample for which low temperature data is available (lower experimental curve in Fig. 5). Using the donor and compensating acceptor concentrations obtained from the analysis of the carrier concentration and the Brooks-Herring formula, we obtain the dotted

curve in Fig. 5. The agreement is satisfactory considering the uncertainties in the data and in the simple application of the theory.

It should be noted that a study of the mobilities of ZnTe and ZnSe will in a general way parallel the corresponding studies of the more thoroughly investigated semiconductors in the III-V compound family. For as Ehrenreich[25] has shown, at least for the n-type materials, the polar character of these semiconductors plays a major role in their transport properties. This would also be expected to be true for the II-VI compounds because of their strongly polar nature. To provide a reasonably complete study of the intrinsic (or lattice) mobility of these materials, four scattering mechanisms should be considered. These are scattering by the piezoelectric activity of the acoustic modes, the deformation potential, and the non-polar and polar interactions with the optical modes. For all four, μ drops off with increasing T. As we will attempt to determine which of these mechanisms contribute appreciably to the observed μ, we will in the following consider each of them separately and in some detail. Unless otherwise indicated, we will avoid the complications arising from the degenerate valence bands (for p-type ZnTe) by the relatively rough approximation of treating them as a simple band. With a suitable m^* this should provide us with results which are at least semi-quantitatively correct; and this is all that will be required for our purposes.

The scattering by piezoelectrically active acoustic modes, first treated by Meijer and Polder[26] and Harrison,[27] results from the small component of polarization present in the long wavelength acoustic modes. The mobility of carriers in a simple band with this interaction is

$$\mu_{piezo} = 1.05\ \rho\ \langle u_\ell^2 \rangle \epsilon_s^2\ e_{14}^{-2}\ (m^*/m)^{-3/2}\ T^{-1/2}\ cm^2/V\ sec. \qquad (4)$$

where ϵ_s is the static dielectric constant, e_{14} the piezoelectric constant (in esu/cm^2), ρ the density, and $\langle u_\ell^2 \rangle$ the square of longitudinal sound velocity averaged over direction. Aside from m^*/m, for which we use the values stated above, the values of the various parameters used in Eq. (4) are given in Table 1. The resulting mobilities are:

$$\mu_{piezo}(ZnTe) \approx 1.6 \times 10^5\ (300/T)^{1/2}\ cm^2/V\ sec.$$

$$\mu_{piezo}(ZnSe) \approx 3.5 \times 10^5\ (300/T)^{1/2}\ cm^2/V\ sec.$$

These values exceed the measured ones by well over a factor of 100 and thus indicate that this mechanism does not play an important role in determining the μ for either of the two materials.

The theory of deformation potential (or acoustic mode) scattering is well known. The mobility for this case can be expressed as

$$\mu_{dp} = 3.0 \times 10^{-5}\ (m^*/m)^{5/2}\ \rho\ \langle u_\ell^2 \rangle\ T^{-3/2}\ E_b^{-2}\ cm^2/V\ sec \qquad (5)$$

where E_b denotes the deformation potential (in eV) for the relevant band edge.[28]

Unfortunately there is no direct information about these quantities for ZnSe and ZnTe. However, information about the pressure coefficients of a fairly large number of semiconductors is available. From the regularity of the pertinent data it appears that estimates of the required quantities can be made which are sufficiently accurate for our purpose. We take the values of 4 ev and 2 ev as the deformation potentials for the conduction band edge of ZnSe and the valence band edge of ZnTe respectively.[29] With these values the calculated mobilities are

$$\mu_{dp}(\text{ZnTe}) = 4 \times 10^3 \, (300/T)^{1/2} \text{ cm}^2/\text{V sec}$$
$$\mu_{dp}(\text{ZnTe}) = 2 \times 10^4 \, (300/T)^{1/2} \text{ cm}^2/\text{V sec}.$$

Since these values are about a factor of 40 times larger than the measured values, it appears that acoustic mode scattering is not important for these compounds. Of course, if the deformation potentials are much larger than our estimated values, (say by a factor of five) our conclusion would be in error. However, it seems rather unlikely in light of present knowledge that these quantities can be so huge.

The expression for the mobility of holes in degenerate p-like bands scattered by the non-polar interaction with the optical phonons, μ_{npo}, can be obtained from the work of Ehrenreich and Overhauser.[30] From their study of the mobility of holes in Ge, it can be readily shown that

$$\mu_{npo} = \frac{1.35 \times 10^{17}}{C_4^2} \frac{\rho a^2 \theta^3}{T^{5/2}} \left[\frac{m^{5/2}(m_1^{1/2} + m_2^{1/2})}{(m_1^{3/2} + m_2^{3/2})^2}\right] \int_0^\infty \frac{x \exp(-\theta T^{-1} x) dx}{\varphi(x^{-1})} \text{ cm}^2/\text{V sec}$$

$$\text{with } \varphi(t) = n(1+t)^{1/2} + (n+1)(1-t)^{1/2} \quad \text{for } t < 1 \qquad (6)$$

$$= n(1+t)^{1/2} \quad \text{for } t > 1.$$

Here n is the usual optical phonon occupation number given by $[\exp(\theta/T) - 1]^{-1}$, θ the Debye temperature, m_1 and m_2 the masses of the light and heavy hole respectively, α the lattice constant (in cm), and C_4 the coupling constant (in eV). The constant C_4 is analogous (but not equal) to the deformation potential for the optical modes in say Conwell's formulation.[31] In line with our limited knowledge about the masses for ZnTe the factor involving the masses is replaced by $m^{*-5/2} = (0.6m)^{-5/2}$. The biggest uncertainty, however, is in the magnitude of the optical mode coupling parameter C_4, about which little is known. To our knowledge the only semiconductor for which the strength of this coupling has been determined is Ge. In their recent study of the mobility of p-type Ge, Brown and Bray[32] have determined coupling parameters for the different modes (so called optical and acoustic deformation potentials). From their results it is possible to deduce that the value of C_4 is 20 eV, which corresponds to their optical mode deformation potential of 8.8 eV. On the other hand it is possible to make a rough estimate of the upper

limit of this parameter for InSb. We find the value to be 15 eV.[33] Using the value of 15 eV for ZnTe we find that μ_{npo} has the values of 790, 2000, and 1800 cm^2/V sec at T = 300°, 200°, and 100°K respectively. These values are too large by a factor of about 8 at 300°K and 25 at 100°K.

With significantly larger values for the mass and C_4 than the estimates that we have used, μ_{npo} could yield values comparable to the observed values. On the other hand it is important to note that the temperature dependence of μ_{npo} also is not in very good accord with the data, as it increases too rapidly with decreasing temperature. Thus while we cannot at present definitely rule out the possibility that this type of scattering contributes significantly to the total, these observations suggest that it doesn't dominate the scattering.

This mechanism can be completely ruled out for n-type ZnSe for two reasons. First, the effective mass is small and $\mu_{npo} \propto (m^*)^{-5/2}$. The second and more important reason is that for the Γ_1 (s-like) conduction band minimum the matrix element for scattering between electronic states k and k' vanishes to lowest order in the phonon wave vector q = k - k'. The reduction in the scattering due to this selection rule is $\sim 10^{-3}$.

The last mechanism to be considered is the scattering of the carriers by the electric polarization associated with the optical

modes. The strength of the interaction is indicated by the polar coupling constant α which is

$$\alpha = (m^*/m)^{1/2} \, (Ry/\hbar\omega_\ell)^{1/2} \, (\epsilon_\infty^{-1} - \epsilon_s^{-1})$$

where Ry is the Rydberg of energy, $\hbar\omega_\ell$ the energy of the longitudinal optical mode for long wavelength, and ϵ_∞ the high frequency or optical dielectric constant.[34] Using the relevant parameters, which are given in Table I and the assumed values of m^*/m we find that $\alpha = 0.41$ and 0.39 for electrons in ZnSe and holes in ZnTe respectively. By noting that the factor which more properly reflects the magnitude of succeeding orders of perturbation is $\alpha/6$, it is evident that the weak coupling approach is probably adequate for these materials. The perturbation theory result for simple parabolic bands obtained by Howarth and Sondheimer[35] and in which the Callen effective charge[36] is used can be written as

$$\mu_{polar} = \frac{0.870(m/m^*)}{\alpha\hbar\omega_\ell} \left[\frac{e^z - 1}{z^{1/2}}\right] G(z)e^{-z} \quad cm^2/V \text{ sec} \qquad (7)$$

where $z = \hbar\omega_\ell/kT = \theta/T$, $\hbar\omega_\ell$ is in eV, and $G(z)e^{-z}$ is a tabulated function. A more general result having the same form as Eq. (7) but in which the screening by the carriers is taken into account was given by Ehrenreich.[37] His G(z) is a function of the carrier concentration through the plasma frequency ω_p defined by $\omega_p^2 = 4\pi e^2 n/m^*$. The difference between the G(z) for the screened and

unscreened interactions vanishes as $\omega_p/\omega_\ell \longrightarrow 0$. Since $\omega_p/\omega_\ell \ll 1$ for all ZnSe and ZnTe crystals considered in this context, the screening can be neglected.

The values obtained from Eq. (7) are shown as the solid curves in Figs. 5 and 6. In contrast to the previous mechanisms considered, polar scattering leads to results which are quite close to the experimental mobilities. It is noteworthy that there are no adjustable parameters in μ_{polar} except perhaps the m^*s (which, in fact, have not been varied). There is an apparent small discrepancy in that the calculated curves exhibit a small positive curvature at the higher temperatures while the data do not. However, as has been found in a recent study of CdTe[38] this can be simply understood in terms of the temperature dependence of the static dielectric constant which has been neglected in the solid curves. A small variation in $\epsilon_s(T)$ has an appreciable effect on α because of the considerable cancellation between ϵ_∞^{-1} and ϵ_s^{-1}. To estimate this effect we have made the assumption that the temperature variation of ϵ_s for ZnTe and ZnSe is similar to that for CdTe. It is to be noted that the dashed curves which include this correction, have a temperature dependence which more closely resembles the data in the intrinsic range.

In summary, the polar optical mode scattering clearly dominates the intrinsic scattering of electrons in ZnSe, the

scattering from all other mechanism being very much weaker. This mechanism is undoubtedly also very important for p-type ZnTe as the estimated mobility due to it alone has the correct magnitude and temperature dependence. The other scattering mechanism that possibly could be important in the scattering of the holes is the non-polar interaction with the optical phonons. This could be the case if the appropriate coupling parameter is considerably larger than the values we have considered. Finally, it should be noted that high temperature data would be very helpful in assessing the roles of these two mechanisms since $\mu_{npo} \propto (\theta/T)^{3/2}$ while $\mu_{polar} \propto (\theta/T)^{1/2}$ for $T \gg \theta$.

IV. CONCLUSION

The present study of the electrical transport properties of ZnSe and ZnTe has shown that shallow impurity states, observed in materials like Si, Ge and the more thoroughly studied compounds of the III-V compound family are more widespread in the II-VI compounds than has been believed in the past. Furthermore, it was found that the processes controlling the electircal conduction of the investigated compounds are similar to those that have been shown to be important in such compounds as InSb and GaAs. Thus, in spite of their less covalent character, the II-VI compounds are in these respects quite similar to the more conventional semiconductors.

The method of firing the crystals in liquid Zn has enabled us, by sufficiently suppressing the concentration of compensating impurity and native defects, to observe a shallow donor level in ZnSe with ionization energy of ~ 0.01 eV. It has also proved possible to prepare heavily Al-doped ZnSe crystals which are degenerate.

The discovery of shallow acceptors in ZnTe represents the first case in which uncompensated acceptor levels of near hydrogenic depths have definitely been observed in any of the II-VI semiconductors. Acceptor levels correlated with Cu, Ag, and Au dopants were identified and found to have ionization energies of 0.15, 0.11 and 0.22 eV respectively. The levels are most probably simple acceptors resulting from the substitutional replacement of Zn atoms by noble metal atoms; although more complex models cannot presently be excluded. A level at 0.048 eV in undoped crystals has been identified as being due to a Zn vacancy. Some evidence is presented for what is believed to be the second charge state of the vacancy.

The Hall mobility data on lightly doped ZnSe and ZnTe strongly suggest that the mobilities for $T \gtrsim 100^{\circ}K$ are determined by the intrinsic properties of the crystals. Analysis of the intrinsic (or lattice) mobility indicates that in the case of ZnSe polar optical mode scattering strongly dominates over the scattering by the piezoelectric activity of the acoustic modes, the deformation

potential, and the non-polar interaction with the optical modes. Similarly, the polar scattering of the optical phonons appears to be the important mechanism determining the mobility of holes in ZnTe. It is possible, however, that the non-polar optical mode interaction could also contribute appreciably to the scattering of the holes if the relevant coupling parameter is significantly larger than the corresponding parameters for Ge and InSb.

TABLE I

Parameters Used in Calculating
Mobilities for ZnSe and ZnTe

	ZnSe	ZnTe
$\epsilon_s (T = 300^{\circ}K)$	8.1[a]	10.1[c]
ϵ_∞	5.75[a]	8.26[c]
$\hbar\omega_\ell$ (eV)	0.0314[a]	0.0259[b]
$e_{14} (\frac{\text{stat. coul.}}{\text{cm}^2})$	1.5×10^4 [d]	8.5×10^3 [d]
$\rho \langle u_\ell^2 \rangle$ $(\frac{\text{dynes}}{\text{cm}^2})$	1.06×10^{12} [e]	8.5×10^{11} [e]

a) reference 4

b) reference 11

c) reference 1

d) D. Berlincourt, H. Jaffe and L. R. Shiozawa, submitted for publication in Phys. Rev.

e) derived from the elastic constants in d.

REFERENCES

1. L. R. Shiozawa et al, Aeronautical Research Laboratory Contract No. AF 33(616)-6865, Final Report, Period Jan. 1960 - Dec. 1961.
2. A. G. Fisher and A. S. Mason, Air Force Cambridge Research Laboratories Contract No. AF 19(604)-8018, Scientific Reports No. 1, 2 and 3 (1961).
3. M. Aven and W. W. Piper, Air Force Cambridge Research Laboratories Contract No. 19(604)-8512, Scientific Report No. 1 (1961).
4. M. Aven, D. T. F. Marple and B. Segall, J. Appl. Phys. 32, 2261 (1961).
5. M. Aven and H. H. Woodbury, Air Force Cambridge Research Laboratories, Contract No. 19(604)-8512, Scientific Report No. 2 (1962).
6. R. H. Bube and E. L. Lind, Phys. Rev. 110, 1040 (1958).
7. M. Aven and H. H. Woodbury, J. Appl. Phys. Ltrs. (Nov. 1962).
8. L. C. Greene, D. C. Reynolds, S. J. Czyzak, and W. M. Baker, J. Chem. Phys. 29, 1375 (1958).
9. W. W. Piper and S. Polich, J. Appl. Phys. 32, 1278 (1961).
10. E. Loh and R. Newman, J. Phys. Chem. Solids, 21, 324 (1961).
11. R. E. Halsted and M. Aven, Bull. Am. Phys. Soc. 6, 312 (1961).
12. D. C. Reynolds, L. S. Pedrotti and O. W. Larson, J. Appl. Phys. 32, 2250 (1961).
13. On the basis of their optical absorption measurements at absorption constants in the range 5 to 100 cm^{-1} Aten et al. (A. C. Aten, C. Z. van Doorn and A. T. Vink, Proceedings of the

International Conference on the Physics of Semiconductors, Exeter, 1962) have concluded that the lowest energy optical transition in ZnTe is indirect. However, at such low values of α the effects of impurities and of phonon assisted direct exciton transition can be important; and it does not appear that these have been adequately studied. In addition, it would be very difficult to understand the occurrence of the sharp emission lines at energies appreciably larger (~ 0.1 eV) than the energy of the indirect gap.

14. J. J. Hopfield and D. G. Thomas, Phys. Rev. 122, 35 (1961).

15. J. O. Dimmock and R. G. Wheeler, J. Appl. Phys. 32, 2271 (1961).

16. See, for example, T. H. Geballe, Semiconductors, edited by N. B. Hannay, Reinhold Publ. Corp., New York (1959), p. 313.

17. R. T. Delves, Proc. Phys. Soc. (London) 73, 572 (1959).

18. S. Teitler and R. F. Wallis, J. Phys. Chem. Solids 16, 71 (1960).

19. This value can be understood by noting that g is the ratio of the number of ways a hole can occupy a singly ionized acceptor to the number of ways a hole can be ionized from a neutral acceptor. Since there are three occupied electronic orbitals in each singly ionized double acceptor (see reference 18) while there are two holes in the neutral state, the ratio is 3/2.

20. In order to get a precise estimate of the ionization energy of the lower level, it was necessary to extend the measurements

for at least one crystal to as low a temperature as possible. This was accomplished by intentionally leaving a small amount of Cu in this crystal, which technique helped to maintain ohmic behavior of the electrical contacts to lower temperatures.

21. Of the possible acceptor elements in ZnTe, the alkali metals, the 3d transition elements and Sb can be ruled out since their concentrations in our samples (as determined by spectroscopic analysis) was too low. P and As, on the other hand, cannot be ruled out on this basis because of their very high limits of detectability. Judging by the available (but admittedly limited) information about these elements in other II-VI compounds (ref. 6), the levels introduced by P and As would probably be much deeper than 0.15 eV.

22. Firing under higher Te pressures led to disintegration of the crystals.

23. It should be noted that crystals grown from undoped ZnSe powder are likely to contain less acceptor impurities than those grown from Cl-doped powders. It has been observed that the presence of halogens during crystal growth tends to favor the incorporation of acceptor impurities by vapor transfer from the original powder charge to the growing crystal boule. (P. Kovács and J. Szabó, paper presented at the International Conference on Luminescence, Balatonvilágos, Hungary, 1961).

24. P. P. Debye and E. M. Conwell, Phys. Rev. 93, 693 (1954).

25. H. Ehrenreich, J. Phys. Chem. Solids 9, 129 (1959); Phys. Rev. 120, 1951 (1960); J. Appl. Phys. 32, 2155 (1961); see also C. Hilsum and A. C. Rose-Innes, Semiconducting III-V Compounds, Pergamon Press, New York, 1961.

26. H. J. G. Meyer and D. Polder, Physica 19, 255 (1953).

27. W. A. Harrison, Phys. Rev. 101, 903 (L) (1956), Thesis Univ. of Illinois (1956).

28. See, for example, H. Brooks, Advances in Electronics and Electron Physics, edited by L. Marton (Acad. Press, New York, 1955) Vol. 7, p. 87.

29. The difference in the deformation potentials for the s-like conduction band and the p-like valence bands is nearly the same (~ 6 eV) for all group IV and III-V semiconductors (see W. Paul, J. Appl. Phys. 32, 2082 (1962)). Thomas' values of 4.5 eV (J. Appl. Phys. 32, 2298 (1961)) and Langer's value of 3.8 eV (to be published) for CdTe suggest that this crude relation also holds for the II-VI compounds. Also, for Ge it has been shown (H. R. Philipp, W. C. Dash, and H. Ehrenreich, Phys. Rev. 127, 763 (1962)) that the deformation potential for the valence band ($\Gamma_{25'}$) edge is opposite and equal to roughly half that for conduction band (Γ_{21}) edge at $\underline{k} = 0$.

30. H. Ehrenreich and A. W. Overhauser, Phys. Rev. 104, 331 and 649 (1956).

31. E. Conwell, J. Phys. Chem. Solids 8, 236 (1959).

32. D. M. Brown and R. Bray, Phys. Rev. 127, 1593 (1962).

33. As C. Hilsum and A. C. Rose-Innes (reference 25) have already noted, polar optical mode scattering apparently accounts for the room temperature hole mobility (750 cm^2/V sec) of InSb. Using this fact, the limit on C_4 is then arrived at by applying Eq. (6) and requiring $\mu_{npo} > 10^3$ cm^2/V sec. A value of $m^* = 0.4$ m (F. Stern, Proceedings International Conference on Semiconductor Physics, Prague 1960, p. 363) was used. The larger values of $m^* = 0.5$ m and 0.6 m suggested by H. Ehrenreich (J. Phys. Chem. Solids 2, 131 (1957)) and Hilsum and Rose-Innes would lead to lower values for C_4.

34. See, for example, A. R. Hutson, Semiconductors, edited by N. B. Hannay, Reinhold Publ. Corp., New York (1959) p. 541.

35. D. J. Howarth and E. H. Sondheimer, Proc. Roy. Soc. (London) A219, 53 (1953).

36. H. Ehrenreich, J. Phys. Chem. Solids 2, 131 (1957).

37. H. Ehrenreich, J. Phys. Chem. Solids 8, 130 (1959).

38. B. Segall, M. R. Lorenz and R. E. Halsted, to be published.

FIGURE CAPTIONS

Fig. 1 Temperature dependence of the Hall coefficient for ZnTe crystals doped with Au (squares), Cu (triangles) and Ag (circles) and for an undoped ZnTe crystal fired in liquid Zn at 900°C (diamonds).

Fig. 2 Temperature dependence of the free hole concentration for a ZnTe crystal found (by chemical analysis) to contain $(2 \pm 1) \times 10^{16}$ cm^{-3} Cu. The data are indicated by circles. The solid line represents the hole concentration calculated from Eq. (1) with $N_a = 3.5 \times 10^{16}$ cm^{-3}, $N_d = 3.1 \times 10^{15}$ cm^{-3} and $E_a = 0.149$ eV.

Fig. 3 Temperature dependence of the hole concentrations for undoped ZnTe crystals fired under various partial pressures of Te. Theoretical curves, calculated from Eq. (3), are indicated by solid lines. The dashed curve represents the low temperature range for the $p_{Te} = 0.26$ atm crystal fitted using Eq. (1) (see text).

Fig. 4 Temperature dependence of the Hall coefficient for ZnSe crystals doped with Cl (diamonds) and Al (squares) and for an undoped ZnSe crystal (circles). The points calculated from Eq. (1) for the undoped crystal, with $N_d = 9.5 \times 10^{16}$ cm^{-3}, $N_a = 8.7 \times 10^{16}$ cm^{-3} and $E_d = 0.008$ eV, are indicated by triangles.

Fig. 5 Temperature dependence of the Hall mobility for an undoped ZnSe crystal with $n_{300^oK} = 6.9 \times 10^{16}$ cm^{-3} (squares), a Cl-doped crystal with $n_{300^oK} = 8.6 \times 10^{16}$ cm^{-3} (triangles) and a Cl-doped crystal with $n_{300^oK} = 6.8 \times 10^{16}$ cm^{-3} (circles). The solid curve represents the calculated mobility for polar scattering of optical phonons. The dashed curve includes an approximate correction for the temperature variation of ϵ_s. The dotted curve is the mobility calculated for charged impurity scattering for the undoped sample.

Fig. 6 Temperature dependence of the Hall mobility for two undoped (circles and squares) and a Ag-doped (triangles) ZnTe crystal. The solid curve represents the calculated mobility for polar scattering of optical phonons. The dashed curve includes an approximate correction for the temperature variation of ϵ_s.

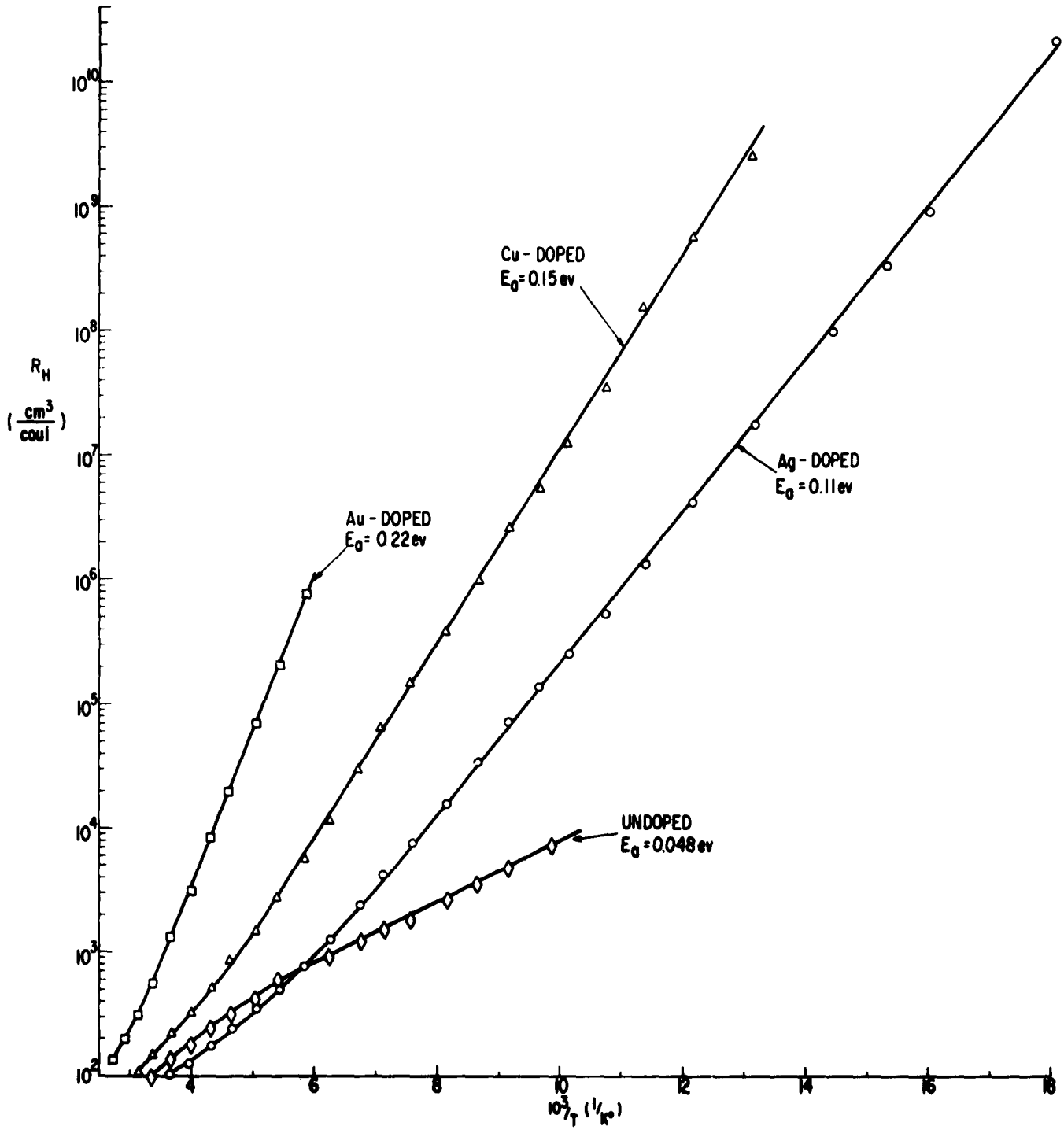
R_H
$(\frac{cm^3}{coul})$
10^{10}
10^9
10^8
10^7
10^6
10^5
10^4
10^3
10^2
Cu - DOPED
E_a = 0.15 ev
Ag - DOPED
E_a = 0.11 ev
Au - DOPED
E_a = 0.22 ev
UNDOPED
E_a = 0.048 ev
4
6
8
10
12
14
16
18
$10^3/_T$ ($^1/_{K^\circ}$)

FIG. 1

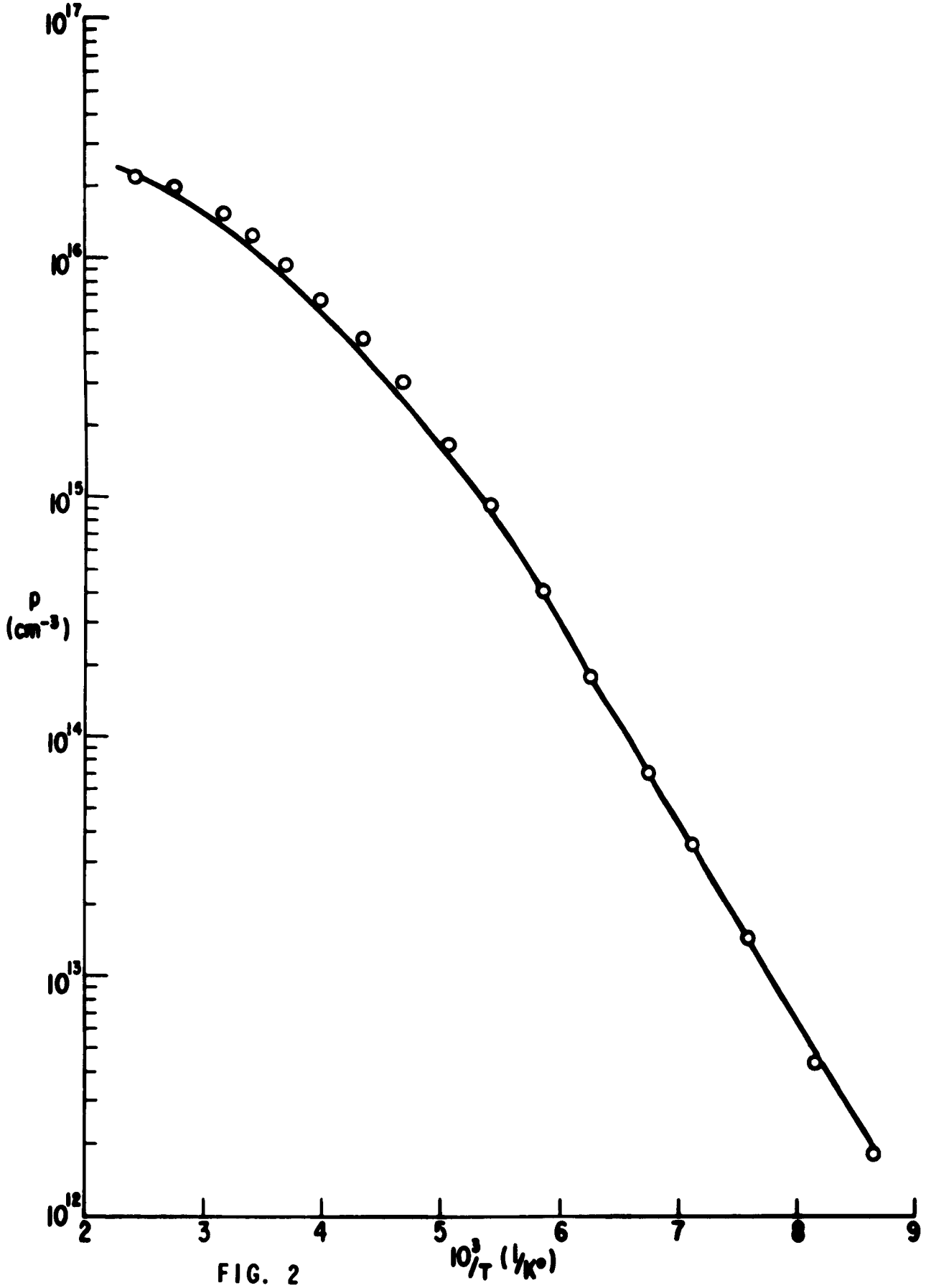

FIG. 2

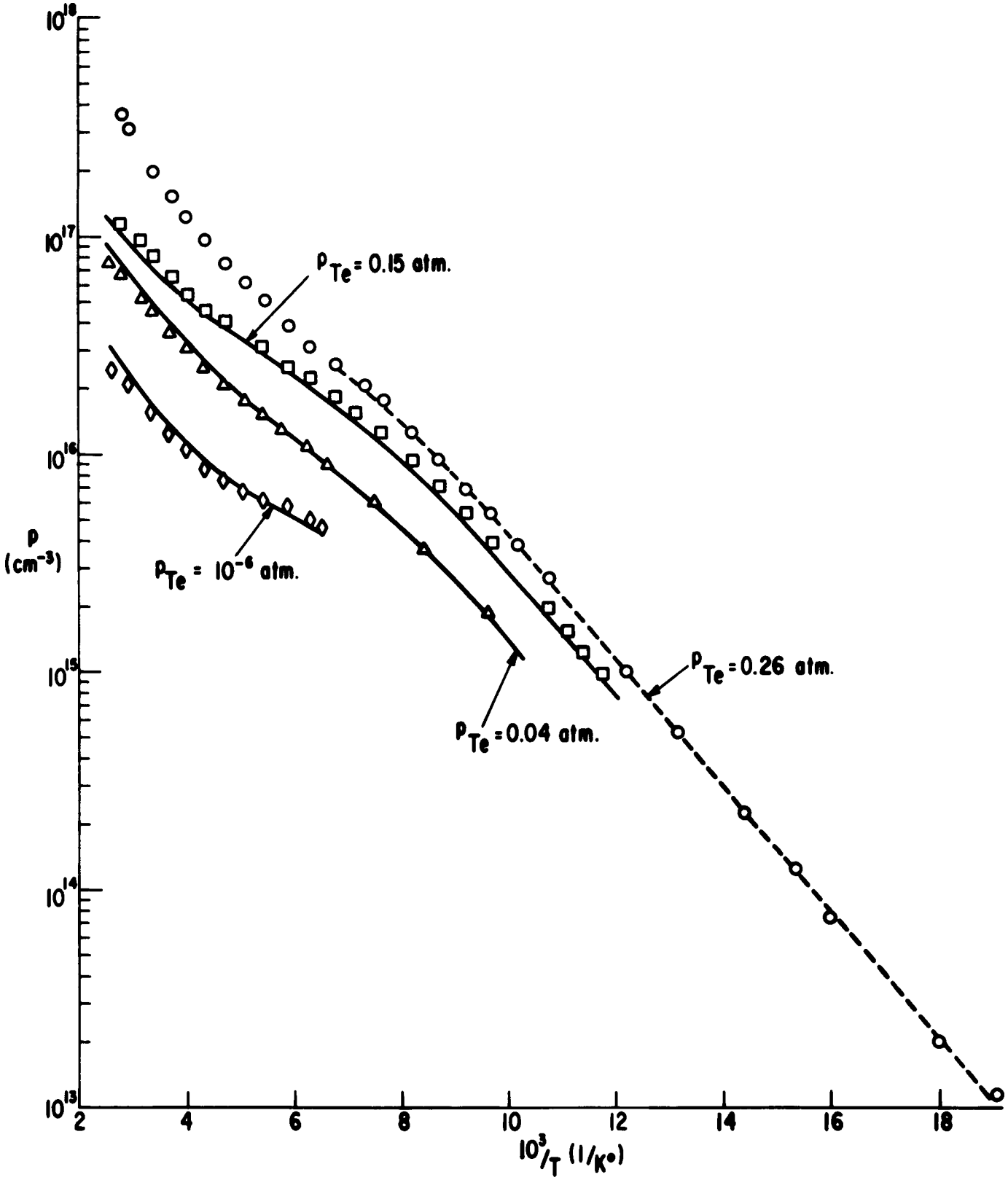
10^{18}
10^{17}
10^{16}
10^{15}
10^{14}
10^{13}
p
(cm^{-3})
p_{Te} = 0.15 atm.
p_{Te} = 10^{-6} atm.
p_{Te} = 0.04 atm.
p_{Te} = 0.26 atm.
2
4
6
8
10
12
14
16
18
$10^3/T$ $(1/K°)$

FIG. 3

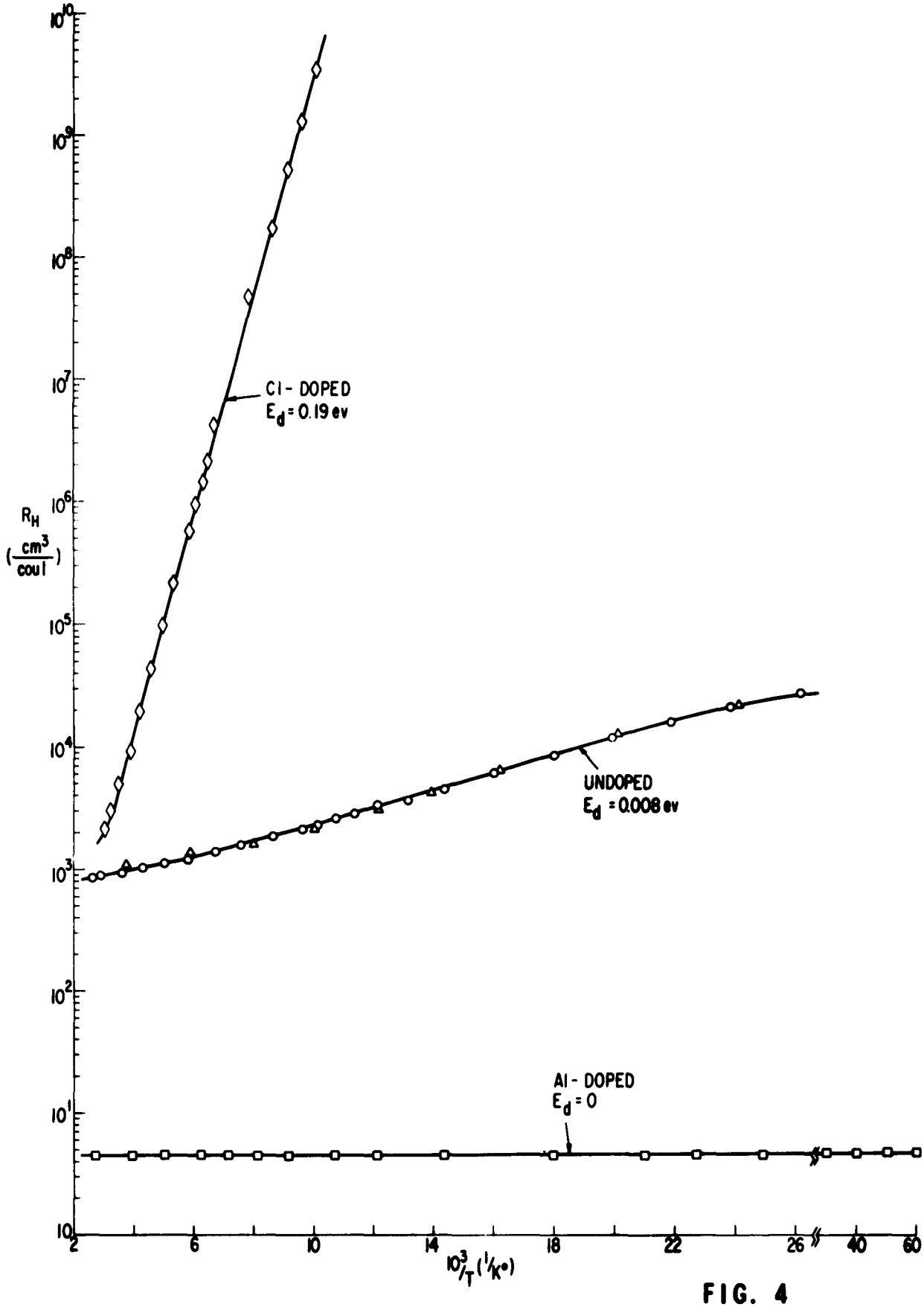
10^{10}
10^{9}
10^{8}
10^{7}
10^{6}
10^{5}
10^{4}
10^{3}
10^{2}
10^{1}
10^{0}
R_H ($\frac{cm^3}{coul}$)
Cl - DOPED
E_d = 0.19 ev
UNDOPED
E_d = 0.008 ev
Al - DOPED
E_d = 0
2
6
10
14
18
22
26
40
60
$10^3/_T$ ($^1/_{K°}$)

FIG. 4

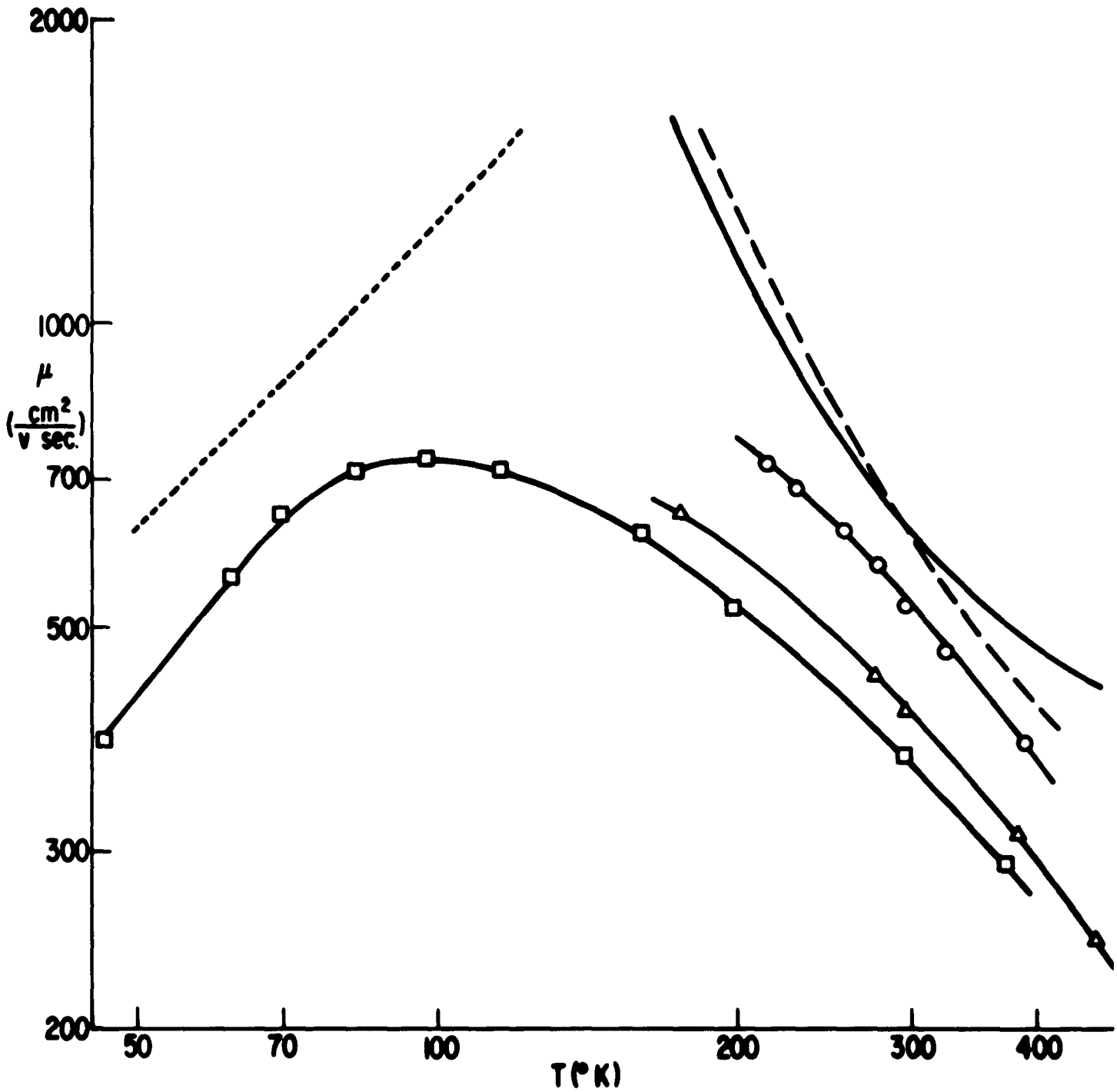

FIG. 5

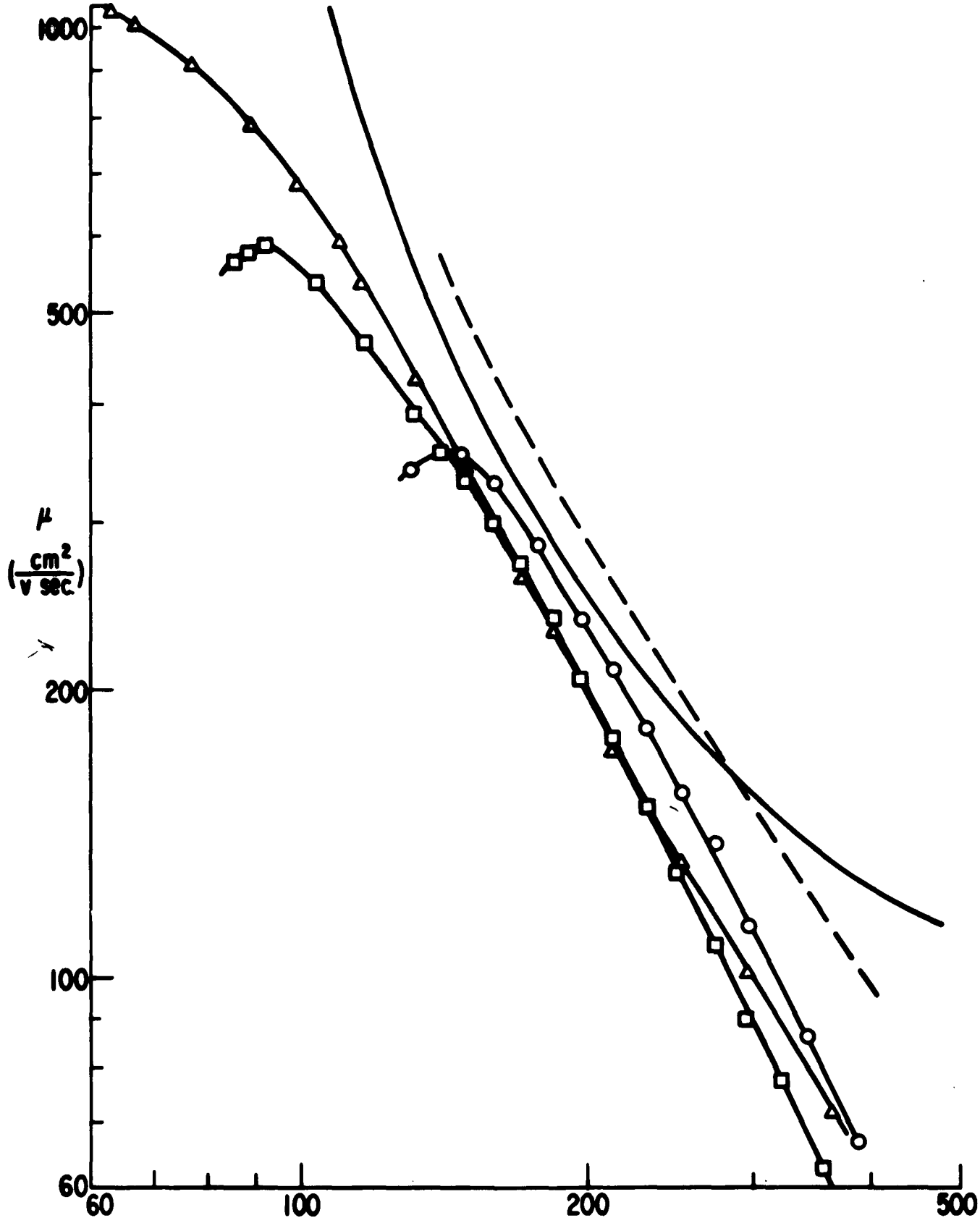

FIG. 6

C. Light Emission From $GaAs_{1-x}P_x$ and GaSb Junctions (J. H. Racette)

Work is continuing on the study of light-emitting $GaAs_{1-x}P_x$ p-n junctions using crystals prepared by growth from a gallium solution, and by halogen transport. The latter crystals were made available to us from another source within the laboratory. It is hoped that these studies will help to improve the reproducibility and luminescence efficiency of these mixed crystal junctions, which are at present unsatisfactory.

Diodes with very good electrical characteristics have been made from zinc diffused (960°C, 1 hour) n-type material. Structures with carefully polished sides have been made with the hope of obtaining laser action, with consequent coherence of the visible junction radiation. As yet, however, sufficiently planar junctions have not been obtained. Presumably this is due to the poor crystal perfection of the n-type bulk material available thus far. The exact location and shape of the junction have been determined either by viewing the radiation produced at the junction, or by preferential etching of the p-type material electrolytically in a 25°/o NaOH solution. Capacitance measurements indicate that the junctions, apart from non-planarity, are somewhat thinner than similarly fabricated GaAs junctions, being typically 300Å wide at zero bias.

The light output of diodes fabricated here has been found to vary linearly with diode current. The spectral distribution of

this radiation has been measured as a function of current at 77°K by J. Kingsley. An appreciable shift to lower wavelength of the peak from 7500Å to 6800Å was observed as the current was increased from 8 to 800 ma for a junction of 0.005 cm^2 area. No line narrowing was noted, the width at half maximum of the energy peak being around 300Å.

Work is also being carried out on GaSb as a radiation source. This is another "direct" material which consequently should yield high efficiency junction recombination radiation.

The procedure used here is the same as that used in connection with $GaAs_xP_{1-x}$. Diodes with polished sides have been fabricated from n-type GaSb into which zinc has been diffused at 660°C for 90 hours.

The radiation from such a junction at 77°K has been measured by W. E. Engeler. A shift of the radiation peak from 1.75μ to 1.70μ was observed as the diode current was varied from 15 ma to 150 ma, the junction area being 0.004 cm^2. Further increase in the current caused only a very slight decrease in wavelength of the peak. The width of this peak at half maximum was found to be about 0.17μ. The radiative output varied linearly with current over most of the range explored, though it increased at a lower rate for low currents. More extensive investigation of this material is planned.

RNH:erm
12/6/62

CONTRIBUTORS

Scientists and technicians who contributed to the work reported:

Staff Members	Technicians
M Aven	W Garwacki
RN Hall	B Binkowski
JH Racette	TJ Soltys
JJ Tiemann	S Schwarz
HH Woodbury	

PAPERS SPONSORED UNDER CONTRACT

R. N. Hall, "Solubility of III-V Compound Semiconductors in Column III LIquids," J. Electrochem. Soc., to be published. Also presented orally at meeting of Electrochem. Soc., Boston, 19 September 1962.

RNH:erm
12/6/62